

Adult Bile Duct Strictures: Role of MR Imaging and MR Cholangiopancreatography in Characterization¹

Venkata S. Katabathina, MD
Anil K. Dasyam, MD
Navya Dasyam, MBBS
Keyanoosh Hosseinzadeh, MD²

Abbreviations: AIDS = acquired immunodeficiency syndrome, AIP = autoimmune pancreatitis, CBD = common bile duct, CHD = common hepatic duct, ERCP = endoscopic retrograde cholangiopancreatography, MIP = maximum intensity projection, MPD = main pancreatic duct, PSC = primary sclerosing cholangitis, RARE = rapid acquisition with relaxation enhancement, RHD = right hepatic duct, RPC = recurrent pyogenic cholangitis, SOD = sphincter of Oddi dysfunction, 3D = three-dimensional, 2D = two-dimensional

RadioGraphics 2014; 34:565–586

Published online 10.1148/rg.343125211

Content Codes:   

¹From the Department of Radiology, University of Texas Health Science Center at San Antonio, San Antonio, Tex (V.S.K.); and Department of Radiology, University of Pittsburgh Medical Center, Presby South Tower, Suite 4895, 200 Lothrop St, Pittsburgh, PA 15213 (A.K.D., N.D., K.H.). Recipient of a Certificate of Merit award for an education exhibit at the 2009 RSNA Annual Meeting. Received December 3, 2012; revision requested February 8, 2013; final revision received June 28; accepted July 1. For this journal-based SA-CME activity, the authors, editor, and reviewers have no financial relationships to disclose. **Address correspondence** to A.K.D. (e-mail: anil.dasyam@gmail.com).

²**Current address:** Department of Radiology, Wake Forest University School of Medicine, Winston-Salem, NC.

See discussion on this article by Taylor (pp 586–588).

SA-CME LEARNING OBJECTIVES

After completing this journal-based SA-CME activity, participants will be able to:

- Discuss the wide spectrum of benign and malignant causes of bile duct strictures in adults.
- Describe salient MR imaging–MR cholangiopancreatographic findings of adult bile duct strictures.
- List the MR imaging–MR cholangiopancreatographic features of the narrowed segment that may help differentiate malignant from benign bile duct strictures.

See www.rsna.org/education/search/RG.

TEACHING POINTS

See last page

Bile duct strictures in adults are secondary to a wide spectrum of benign and malignant pathologic conditions. Benign causes of bile duct strictures include iatrogenic causes, acute or chronic pancreatitis, choledocholithiasis, primary sclerosing cholangitis, IgG4-related sclerosing cholangitis, liver transplantation, recurrent pyogenic cholangitis, Mirizzi syndrome, acquired immunodeficiency syndrome cholangiopathy, and sphincter of Oddi dysfunction. Malignant causes include cholangiocarcinoma, pancreatic adenocarcinoma, and periampullary carcinomas. Rare causes include biliary inflammatory pseudotumor, gallbladder carcinoma, hepatocellular carcinoma, metastases to bile ducts, and extrinsic bile duct compression secondary to periportal or peripancreatic lymphadenopathy. Contrast material–enhanced magnetic resonance (MR) imaging with MR cholangiopancreatography is extremely helpful in the noninvasive evaluation of patients with obstructive jaundice, an obstructive pattern of liver function, or incidentally detected biliary duct dilatation. Some of these conditions may show characteristic findings at MR imaging–MR cholangiopancreatography that help in making a definitive diagnosis. Although endoscopic retrograde cholangiopancreatography with tissue biopsy or surgery is needed for the definitive diagnosis of many of these strictures, certain MR imaging characteristics of the narrowed segment (eg, thickened wall, long-segment involvement, asymmetry, indistinct outer margin, luminal irregularity, hyperenhancement relative to the liver parenchyma) may favor a malignant cause. Awareness of the various causes of bile duct strictures in adults and familiarity with their appearances at MR imaging–MR cholangiopancreatography are important for accurate diagnosis and optimal patient management.

©RSNA, 2014 • radiographics.rsna.org

Introduction

Biliary stricture is a fixed narrowing of a focal segment of the bile duct that results in proximal biliary dilatation and clinical features of obstructive jaundice. A wide spectrum of hepatobiliary and pancreatic diseases, both benign and malignant, can result in the development of biliary strictures (Table 1). It is important to differentiate malignant from benign strictures, since their treatment and prognosis vary. Noninvasive imaging techniques such as ultrasonography (US), computed tomography (CT), and magnetic resonance (MR) imaging play an important role in the evaluation of patients with suspected biliary stricture. Among these techniques, contrast material–enhanced MR imaging with MR cholangiopancreatography offers the most comprehensive evaluation (1,2). Although endoscopic retrograde cholangiopancreatography (ERCP) with tissue biopsy or surgery is needed for the definitive diagnosis of many biliary strictures, certain MR imaging–MR cholangiopancreatographic features of the narrowed segment may help differentiate malignant from benign causes.

In this article, we review the spectrum of bile duct strictures in adult patients and discuss the MR imaging and MR cholangiopancreatographic findings, with emphasis on differentiation between benign and malignant strictures.

Pathophysiologic Features of Bile Duct Strictures

Pathophysiologic mechanisms underlying the development of biliary strictures are different in benign and malignant conditions. Injury to the bile ducts is the inciting event in the development of benign bile duct strictures (3). Inflammatory response follows the injury, resulting in collagen deposition, fibrosis, and focal narrowing, leading to stricture formation (3). The injury may be a single event (eg, trauma during surgery, blunt trauma, deceleration-related trauma, or penetrating abdominal trauma), or it may be a recurring condition such as pancreatitis or PSC. There may be a single stricture or multiple strictures depending on the type of injury. Biliary insults from ischemia are termed ischemic-type biliary lesions. The pathogenesis of these lesions is multifactorial, but prominent components include injury to the cholangiocytes, either directly or as a consequence of damage to arterioles of the peribiliary vascular plexus, leading to stricture formation (4). Sequelae of chronic high-grade strictures may result in atrophy of the hepatic segment or lobe drained by the corresponding bile ducts (5). Malignant bile duct strictures may be secondary to primary bile duct carcinomas such as cholangiocarcinoma, or to extrinsic compression and invasion by malignancies of the adjacent organs such as the gallbladder, liver, and pancreas (3). Extrinsic compression or invasion by porta hepatis lymph nodes and invasion by bile duct metastases may on occasion cause malignant strictures.

MR Imaging—MR Cholangiopancreatographic Technique for Biliary Tract Evaluation

High soft-tissue contrast resolution and the ability to help accurately assess the extent of peripheral ductal involvement are the major advantages of MR imaging. MR cholangiopancreatographic techniques involve the use of heavily T2-weighted sequences to accentuate the high signal from relatively static fluid in the biliary tract while suppressing the signal from background tissues, including flowing blood (Table 2) (6,7). **Either rapid acquisition with relaxation enhancement (RARE) or a variant thereof (eg, single-shot fast spin-echo, half-Fourier acquisition single-shot turbo spin-echo, or fast-recovery fast spin-echo) is used for MR cholangiopancreatography (7).** MR cholangiopancreatographic images can be

Table 1: Hepatobiliary and Pancreatic Diseases Causing Biliary Strictures

Benign conditions
Iatrogenic causes
Pancreatitis
Cholelithiasis
PSC
IgG4-related sclerosing cholangitis
Liver transplantation
RPC
Mirizzi syndrome
AIDS cholangiopathy
SOD
Malignant conditions
Cholangiocarcinoma
Pancreatic adenocarcinoma
Ampullary and periampullary carcinomas
Miscellaneous and rare causes
Biliary inflammatory pseudotumor
Gallbladder carcinoma
Hepatocellular carcinoma
Metastatic disease to bile ducts
Periportal and peripancreatic lymphadenopathy

Note.—AIDS = acquired immunodeficiency syndrome, PSC = primary sclerosing cholangitis, RPC = recurrent pyogenic cholangitis, SOD = sphincter of Oddi dysfunction.

obtained using either of two different techniques: (a) standard two-dimensional (2D) MR cholangiopancreatography, or (b) three-dimensional (3D) isotropic MR cholangiopancreatography (7). Standard 2D MR cholangiopancreatographic protocols generally consist of the thick-slab single-section sequence derived from a breath-hold single-shot RARE technique (8,9). A thick-slab (40–90-mm thickness) single-section heavily T2-weighted RARE sequence (echo time >700 msec) yields ERCP-like projectional images of the entire biliary tree, thereby providing an overview of the anatomy and helping identify the presence and site of the obstruction (Fig 1). Additional radially oriented coronal oblique 2D thick-slab images can be acquired with the patient holding the breath and are helpful when part of the anatomy is obscured by overlapping structures (eg, fluid in the duodenal bulb obscuring the distal CBD) on a single projection. State-of-the-art 3D isotropic MR cholangiopancreatography is performed using a fast-recovery 3D RARE sequence (eg, 3D fast-recovery fast spin-echo), which has two added features compared with standard RARE, including fast recovery and parallel imaging (7). With this sequence, the repetition time is greatly

Table 2: MR Imaging and MR Cholangiopancreatographic Parameters for Evaluation of Biliary Strictures

Parameter	Imaging Sequence					
	Coronal T2W Breath-hold	Axial T2W Breath-hold	2D Thick-Slab MRCP Breath-hold	3D MRCP Respiratory-triggered	Axial T1W FS Breath-hold	Axial/Coronal Multiphase DCE Breath-hold
Pulse sequence	Single-shot fast SE	Single-shot fast SE	Single-shot fast SE	Fast-recovery fast SE	FSPGR	3D GRE/LAVA
Repetition time (msec)	1200	1200	2000–2500	3000–4000	185	4.6
Echo time (msec)	90	90	900	600–700	2.5	2.0
Receiver bandwidth (kHz)	31.25	31.25	25	31.25	41.67	62.50
Field of view (cm)	36	36	30	32	36	40
Section thickness (mm)	5	5	40	0.7 (1.4 with 50% overlap)	5	2.3 (4.6 with 50% overlap)
Intersection gap (mm)	1	1	0	...	1	...
Matrix size	256 × 256	256 × 256	320 × 256	256 × 256	256 × 160	288 × 192
Flip angle (degrees)	90	90	90	90	70	12

Note.—DCE = dynamic contrast-enhanced, FS = fat-saturated, FSPGR = fast spoiled gradient-echo, GRE = gradient-recalled echo, LAVA = liver acquisition with volume acceleration, MRCP = MR cholangiopancreatography, SE = spin-echo, T1W = T1-weighted, T2W = T2-weighted.



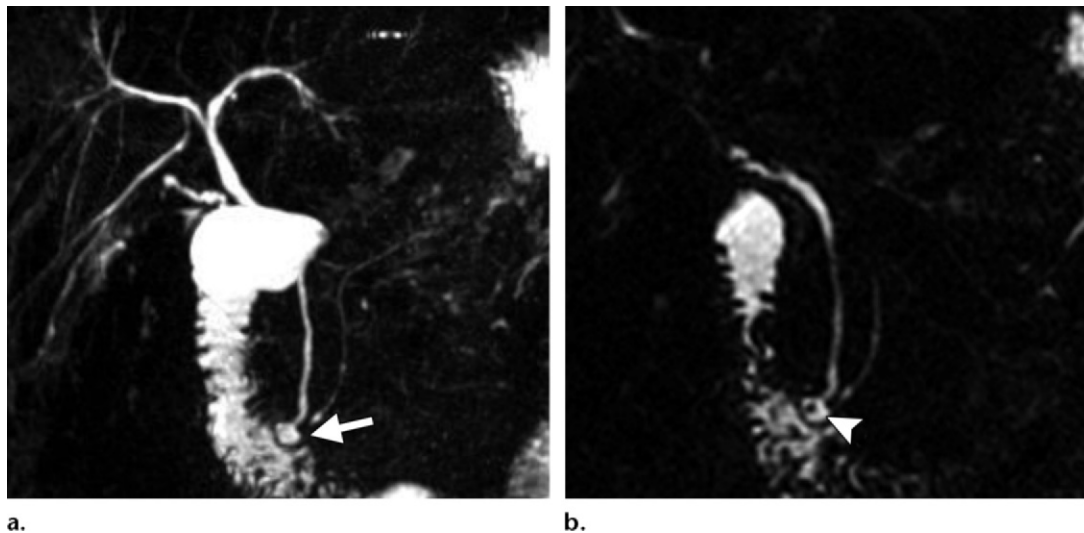
Figure 1. Pancreatic adenocarcinoma in a 48-year-old man. Thick-slab single-section 2D RARE MR cholangiopancreatographic image shows dilatation of the common bile duct (CBD) and MPD (arrows) with abrupt termination at the level of the pancreatic head (arrowhead). Two-dimensional MR cholangiopancreatography typically yields ERCP-like projectional images of the biliary tree, thereby providing an overview of the anatomy.

reduced by using multiple 90° pulses to accelerate the recovery of longitudinal magnetization back to the longitudinal axis rather than depending on T1 relaxation for this process, resulting in short imaging times and increased signal-to-noise ratio. When used in conjunction with parallel imaging (combining imaging data from multiple receiver coils rather than a single coil), the imaging time is further reduced, along with an increase in spatial resolution that permits improved evaluation of intraductal contents and small intrahepatic biliary branches (10). At our institution, we typically use a respiratory-triggered 3D fast-recovery fast spin-echo sequence with

a 1.4-mm section thickness, 50% overlap, and a 256 × 256 matrix interpolated to a 512 × 512 matrix in all directions. Multidimensional images of the entire biliary tract and the pancreatic duct may be obtained by processing 3D isotropic MR cholangiopancreatographic data; maximum intensity projection (MIP), multiplanar reformatting, and volume-rendered images are commonly generated. It is essential to review the 3D source images to assess subtle abnormalities such as very small stones in the CBD (Fig 2).

In addition, a thin multisection sequence is performed in the axial, coronal, and sagittal planes with single-shot RARE (echo time <180 msec) with contiguous or interleaved 3–5-mm sections, which is extremely useful in assessing intraductal disease (7). The shorter echo time also allows evaluation of the duct wall and the periductal anatomy, which can provide important clues as to

Figure 2. Choledochoceles and intraductal calculi in a 40-year-old woman. **(a)** MIP image from a 3D RARE MR cholangiopancreatographic study demonstrates focal dilatation of a short segment of the distal CBD (arrow), a finding that is compatible with a small type III choledochal cyst or choledochoceles. **(b)** Coronal thin-section source image shows a choledochoceles containing a small calculus (arrowhead) that was not discernible on the MIP image.



the cause of biliary strictures. Precontrast T1- and T2-weighted images are useful in the evaluation of the bile duct walls, peribiliary or periportal masses or collections, and hepatic and pancreatic parenchymal diseases. Gadolinium-based contrast-enhanced images aid in further characterization of the narrowed bile duct segment and hepatic and pancreatic focal lesions (9,11,12). Hepatocyte-specific MR contrast agents such as gadolinium ethoxybenzyl diethylenetriamine pentaacetic acid (Gd-EOB-DTPA) can be used. Because up to 50% of this contrast material is actively taken up by functioning hepatocytes and excreted into the biliary tree, delayed phase imaging with these contrast agents can help distinguish partial from complete biliary obstructions (13).

What the Clinician Expects from MR Imaging of the Biliary Tract

The expectations of the referring physician when considering MR imaging in a patient with suspected biliary obstruction include (a) confirmation of the obstruction; (b) exclusion of the other causes of jaundice; and (c) determination of the level of obstruction (intra- or extrahepatic ducts), approximate length of the biliary stricture, and status of the proximal bile ducts. MR cholangiopancreatographic images provide gastroenterologists with a “road map” for planning ERCP or percutaneous transhepatic cholangiography (PTC). Knowledge of the number, location, and length of the strictures may help in selecting the appropriate stent. When possible, the nature of the stricture (benign versus malignant) and the presence or absence of intraductal calculi need

to be addressed. Determination of the extent and stage of the disease process and assessment for the utility of surgery or an interventional procedure are also important for optimal patient care.

Pseudostrictures

Biliary pseudostrictures on MR cholangiopancreatographic images may be patient related or secondary to MR imaging technique or postprocessing-related factors (7). Common causes of pseudostrictures include blooming artifact due to cholecystectomy clips and pulsation artifact from the hepatic artery (Figs 3, 4) (7,14,15). In addition, MR imaging technique-related factors such as incomplete volume acquisition or incorrect reconstruction of a subvolume of ductal data may also contribute to the appearance of a pseudostricture at MR cholangiopancreatography (14). Careful review of axial images obtained during both precontrast and postcontrast phases and of the source data of the 3D RARE MR cholangiopancreatographic images will help avoid misinterpretation of the normal biliary tract as a pseudostricture and unnecessary biliary intervention.

Benign Biliary Strictures

Iatrogenic Causes

The most common cause of a benign biliary stricture is prior hepatobiliary surgery (up to 80%–90% of cases) (16,17). Cholecystectomy is the surgical procedure that most commonly results in strictures of the extrahepatic bile ducts. The prevalence of major bile duct injury

Figure 3. Pseudostricture of the common hepatic duct (CHD) secondary to vascular impression in a 33-year-old woman. **(a)** Thick-slab single-section 2D RARE MR cholangiopancreatographic image shows a short-segment stricture of the proximal CHD (arrow) without intrahepatic biliary dilatation. **(b)** Axial contrast-enhanced MR image at the level of the porta hepatis shows the common hepatic artery (arrow) crossing the proximal CHD (arrowhead), resulting in a pseudostricture.

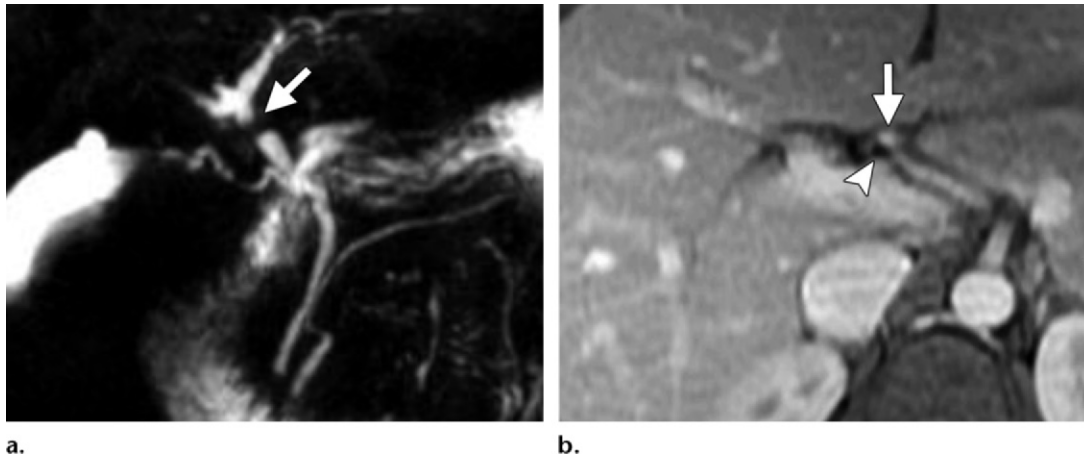
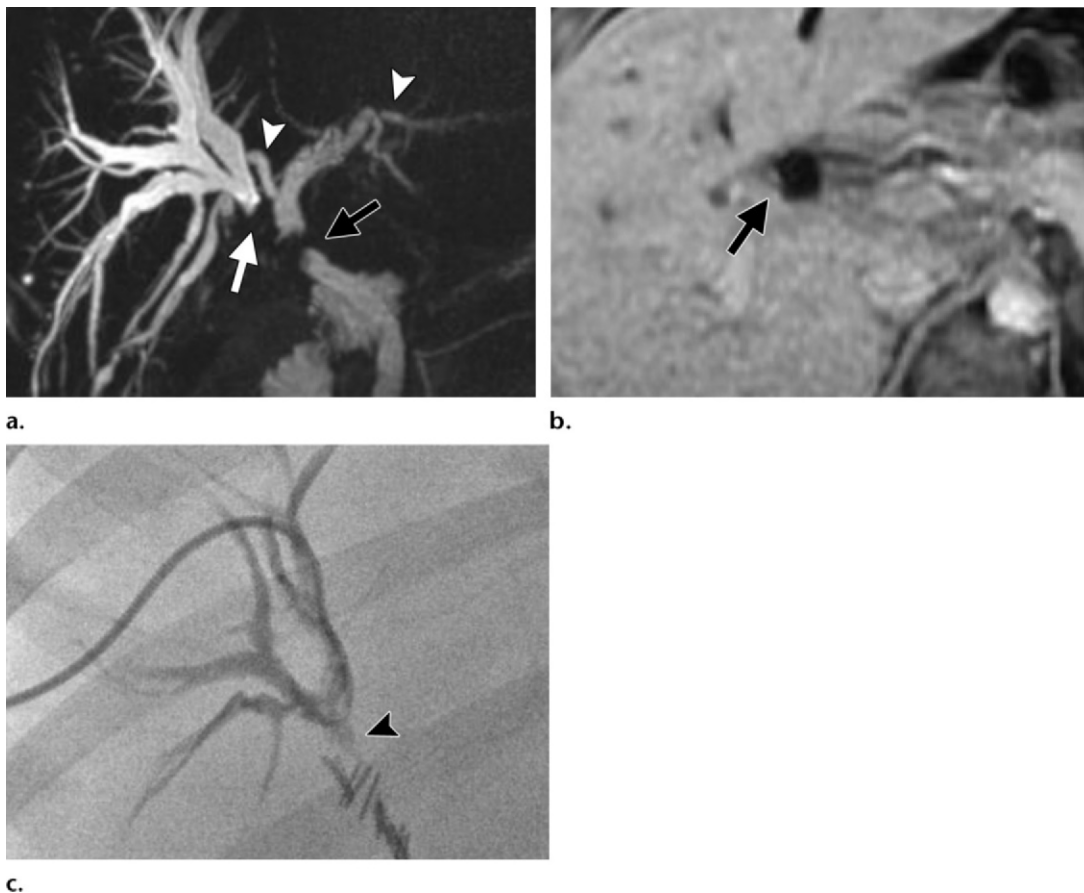


Figure 4. Pseudostricture of the CHD and true stricture of the right hepatic duct (RHD) in a 25-year-old woman who had recently undergone laparoscopic cholecystectomy. **(a)** MIP image from a 3D RARE MR cholangiopancreatographic study shows an apparent focal stricture of the CHD (black arrow), with a normal-caliber left hepatic duct and an aberrant right posterior segmental duct (arrowheads) draining into it. Note also the focal stricture of the right anterior segmental duct (white arrow) with associated upstream biliary ductal dilatation. **(b)** Axial contrast-enhanced MR image demonstrates susceptibility artifact related to cholecystectomy clips at the level of the CHD (arrow), a finding that confirms the presence of a pseudostricture. **(c)** Spot image from a PTC study shows total occlusion of the right anterior segmental duct (arrowhead), consistent with an iatrogenic stricture.



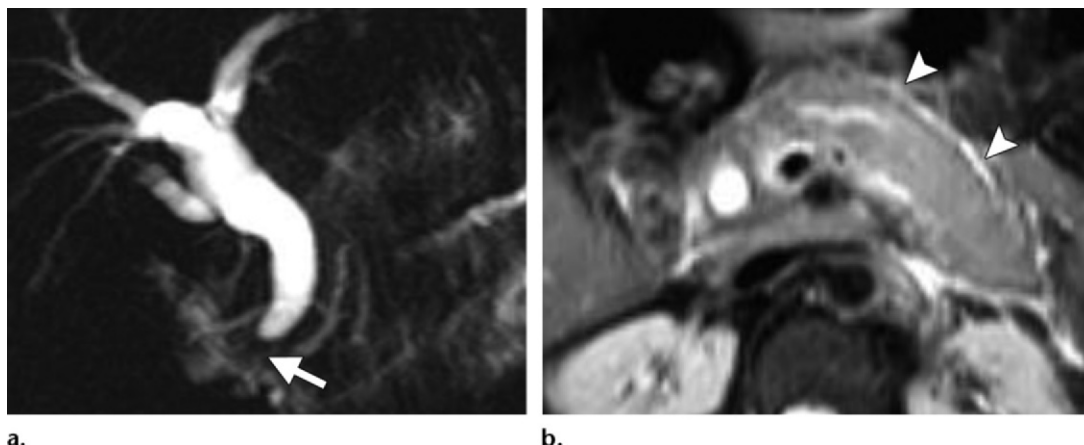


Figure 5. Acute pancreatitis and distal CBD stricture in a 42-year-old man. **(a)** Two-dimensional thick-slab RARE MR cholangiopancreatographic image demonstrates focal narrowing of the distal CBD (arrow) with associated upstream biliary dilatation. **(b)** Axial T2-weighted MR image shows peripancreatic fluid and fat stranding (arrowheads), findings that are consistent with acute pancreatitis.

is 0%–0.5% for open cholecystectomy and up to 1.2% for laparoscopic cholecystectomy (18). The most common locations of postcholecystectomy strictures include the junction of the cystic duct with the CHD and the confluence of the left and right hepatic ducts (19). Potential risk factors for bile duct injury during surgery include aberrant biliary anatomy; inflammation in the hepatobiliary (Calot) triangle (anatomic space bordered by the CHD medially, the cystic duct inferiorly, and the cystic artery superiorly); intraoperative bleeding; and technical factors such as obesity and adhesions (20,21). MR cholangiopancreatography is as sensitive as direct cholangiography and typically shows a short-segment smooth stricture of the CHD or CBD with associated intrahepatic biliary dilatation (Fig 4) (21,22). An iatrogenic stricture can appear to be long if there is complete transection of a bile duct. However, MR cholangiopancreatography may lead to overestimation of the length of the stricture, especially when the duct immediately distal to the stricture is collapsed, rather than truly narrowed (21). At contrast-enhanced MR imaging, the narrowed segment commonly demonstrates a thin, nonenhancing wall with smooth margins (23). Strictures in liver transplant recipients will be discussed later.

Pancreatitis

Chronic pancreatitis accounts for about 10% of all benign biliary strictures, and the prevalence of strictures in patients with chronic pancreatitis varies from 3% to 46% (24). The intrapancreatic portion of the CBD is most commonly involved due to fibrosis of the periductal pancreatic parenchyma (24). Although uncommon, strictures

secondary to mass effect may also develop in acute pancreatitis. MR cholangiopancreatography shows a smooth stricture in the distal CBD with gradual tapering or, less frequently, more abrupt narrowing due to an ultrashort stricture of the terminal CBD (Fig 5) (25). In addition, MR imaging may show changes of acute pancreatitis (enlarged pancreas, peripancreatic fat stranding, and fluid collections) or chronic pancreatitis (parenchymal fibrosis, atrophy, and pancreatic duct dilatation) (Fig 6) (26).

Biliary tract involvement in autoimmune pancreatitis (AIP) merits special mention and will be discussed under “IgG4-related Sclerosing Cholangitis.”

Choledocholithiasis

Choledocholithiasis may occur in 8%–18% of patients with symptomatic gallstones (27). Chronic inflammation secondary to persistent biliary calculi may result in scarring and stricture formation. Given its high sensitivity and specificity, MR cholangiopancreatography is ideally suited for the investigation of CBD calculi (2,28). At MR cholangiopancreatography, bile duct calculi appear as multiple filling defects with angular margins (2,29). In addition, MR imaging with MR cholangiopancreatography may demonstrate associated CBD strictures in chronic choledocholithiasis. Strictures in these patients are usually of the short-segment variety and can occur both above and below calculi in the CBD (Fig 7) (30). Minimal wall thickening and enhancement of the narrowed segment can also be appreciated. Patients with chronic choledocholithiasis and strictures are prone to cholestasis, cholangitis, additional stone formation, and biliary cirrhosis (27,30).

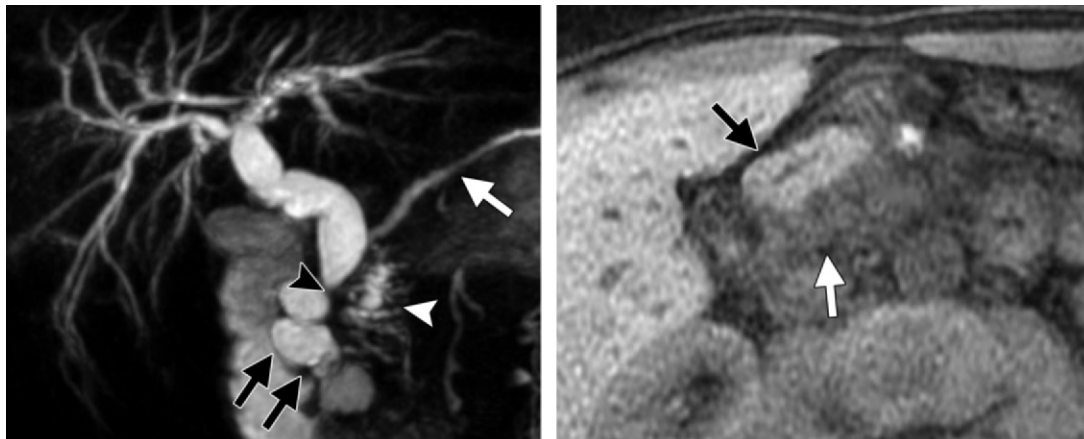


Figure 6. Pancreas divisum and chronic pancreatitis isolated to the ventral anlage in a 43-year-old man. **(a)** MIP image from a 3D RARE MR cholangiopancreatographic study shows a normal-caliber MPD (white arrow), tortuosity and dilatation of the duct of Wirsung and its side branches (white arrowhead), and a focal stricture of the distal CBD (black arrowhead). Note the pancreatic pseudocysts (black arrows) in the pancreaticoduodenal groove. **(b)** On an axial frequency-selective fat-suppressed T1-weighted MR image, the dorsal anlage of the pancreas has normal signal intensity (black arrow), whereas the ventral pancreatic anlage (white arrow) is hypointense secondary to chronic pancreatitis.

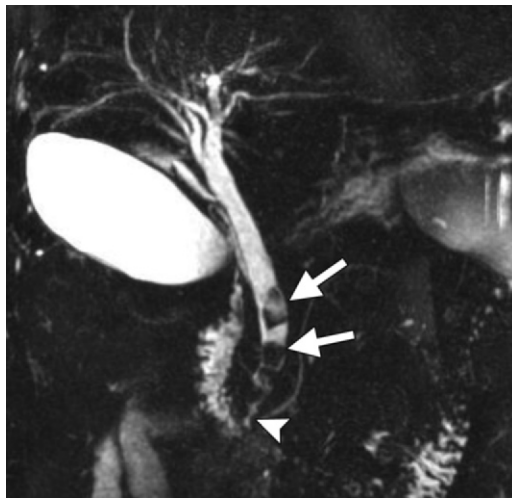


Figure 7. Distal CBD stricture and choledocholithiasis in an 80-year-old man. MIP image from a 3D RARE MR cholangiopancreatographic study demonstrates multiple calculi in the CBD (arrows) with an associated focal short-segment distal CBD stricture (arrowhead).

Primary Sclerosing Cholangitis

PSC is a chronic cholestatic disease of unknown cause that is characterized by inflammatory and obliterative fibrosis of the intra- and extrahepatic bile ducts, and that may progress to hepatic failure and cirrhosis. Approximately 75% of PSC patients have associated inflammatory bowel disease, predominantly ulcerative colitis. Although the exact cause of PSC is unknown, an autoimmune cause is suspected given the association with other autoimmune diseases such as mediastinal and retroperitoneal fibrosis and Sjögren syndrome (31). MR imaging and MR cholangiopancreatography are helpful in determining the status of the bile ducts, characterizing the morphologic features of the hepatic parenchyma, and evaluating for the development

of cholangiocarcinoma (32). MR cholangiopancreatographic findings of PSC include *(a)* multifocal short-segment strictures of the intra- and extrahepatic ducts alternating with normal or mildly dilated ducts, giving rise to a “beaded” appearance; and *(b)* peripheral pruning of the intrahepatic ducts. Hepatic parenchymal abnormalities include peripheral wedge-shaped or reticular T2-hyperintense abnormalities, hypertrophy of the caudate lobe and medial segment of the left lobe with atrophy of the lateral and posterior segments, and large regenerating nodules (Fig 8) (33). Contrast-enhanced MR imaging may show multifocal wall thickening and enhancement of the bile ducts, as well as multiple enhancing areas of fibrosis in the liver periphery. Periportal lymph nodes and intrahepatic duct stones may also be seen (34). Other entities that closely mimic PSC include ascending cholangitis (when associated with strictures and intra-ductal stones), RPC, AIDS cholangiopathy, and ischemic strictures. Cholangiocarcinoma may cause complications in about 10%–15% of PSC patients and should be suspected if the patient develops pruritus, worsening of jaundice, and rapidly increasing serum levels of alkaline phosphatase and bilirubin (31). The carbohydrate antigen 19–9 (CA 19–9) level is often elevated

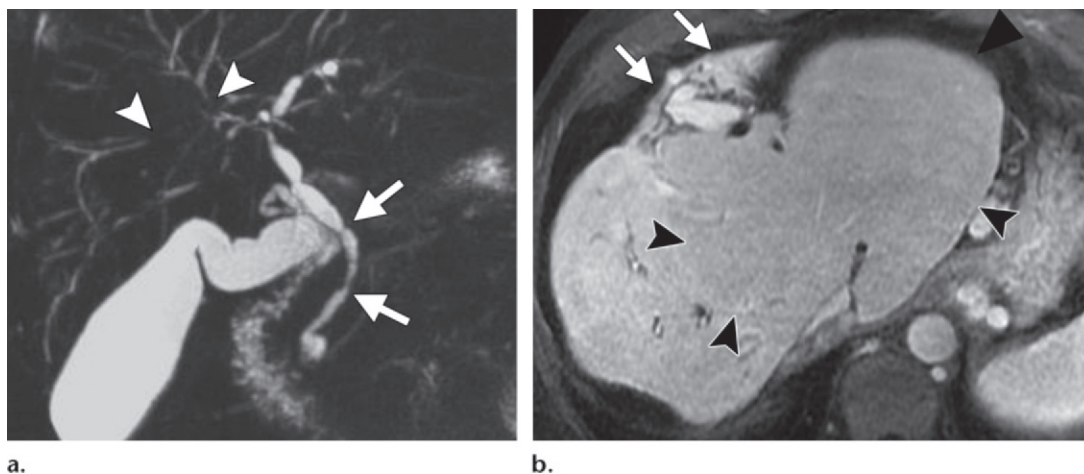


Figure 8. PSC in a 63-year-old man. **(a)** MIP image from a 3D RARE MR cholangiopancreatographic study shows multiple strictures of the CBD interspersed with focal dilations, creating a beaded appearance (arrows), along with multiple discontinuous strictures of the intrahepatic bile ducts involving both hepatic lobes (arrowheads). **(b)** Axial postcontrast MR image demonstrates the typical hepatic morphology of advanced PSC: peripheral hepatic atrophy, particularly involving the left lobe (arrows), and central hypertrophy with a markedly enlarged caudate lobe (arrowheads), giving the liver a lobulated rather than nodular contour.

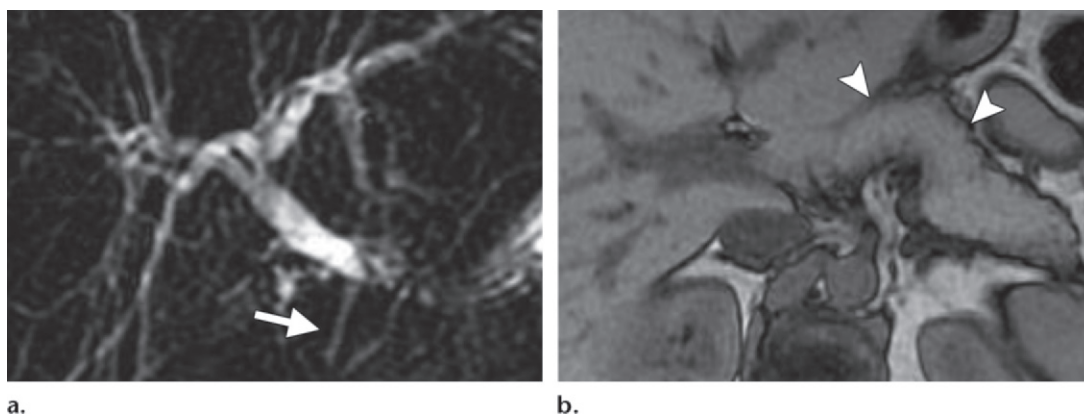


Figure 9. IgG4-related sclerosing cholangitis in a 51-year-old woman. The patient had a history of right upper quadrant pain, jaundice, and elevated serum IgG4 levels. **(a)** Two-dimensional thick-slab RARE MR cholangiopancreatographic image shows a long-segment smooth stricture involving the distal CBD (arrow) with associated upstream biliary dilatation. **(b)** Axial out-of-phase T1-weighted MR image demonstrates normal pancreatic parenchyma (arrowheads) with no evidence of AIP.

in patients who develop cholangiocarcinoma and has a sensitivity and specificity of 78.6% and 98.5%, respectively, with use of a cutoff value of 129 IU/mL (35). However, the CA 19-9 level has a somewhat low positive predictive value of 56.6% and may not be very helpful in identifying cholangiocarcinoma in the early stages. In addition, false-positive elevated levels may be seen with acute bacterial cholangitis and cholestasis (35). MR imaging findings such as a dominant stricture that manifests as high-grade ductal narrowing with markedly dilated proximal ducts, polypoid intraductal masses, and rapid progression of strictures should raise suspicion for cholangiocarcinoma (31,36).

IgG4-related Sclerosing Cholangitis

IgG4-related sclerosing cholangitis is the biliary manifestation of IgG4 sclerosing disease, a recently recognized disease entity that manifests histologically as infiltration by abundant IgG4-positive plasma cells (37). **IgG4 sclerosing disease can result in four different patterns of biliary strictures:** (a) stricture of the distal CBD (Fig 9), (b) diffuse strictures of the intra- and extrahepatic bile ducts, (c) hilar stricture and distal CBD stricture, and (d) isolated hilar stricture (38). MR cholangiopancreatography best demonstrates the presence and distribution of the strictures, whereas cross-sectional MR imaging often shows a thick, symmetric circumferential rind of enhancing tissue surround-

Teaching
Point

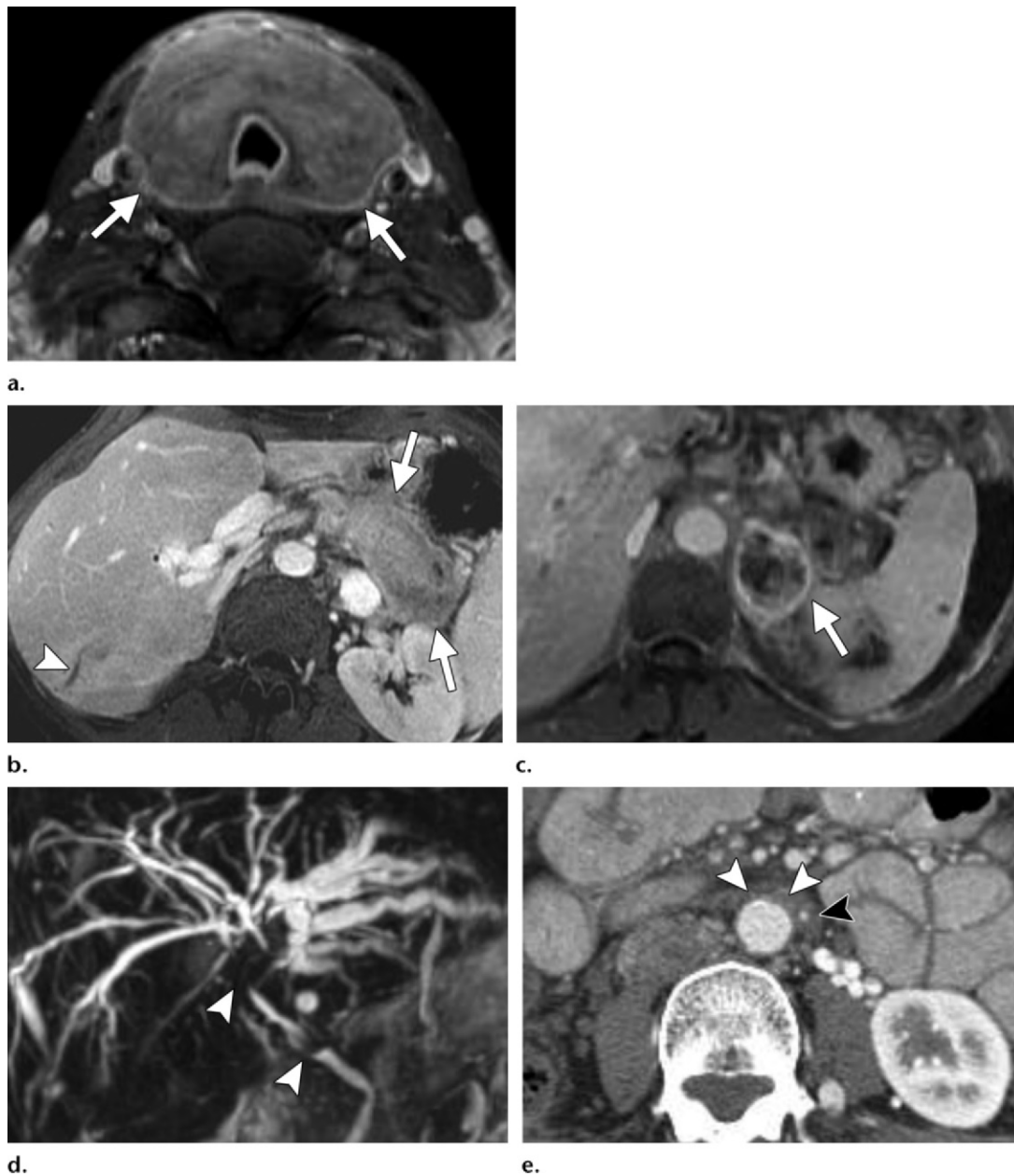


Figure 10. IgG4 sclerosing disease in a 42-year-old woman who initially underwent workup for an anterior neck mass. An adrenal mass and a pancreatic mass were incidentally detected. **(a)** Axial postcontrast T1-weighted MR image shows a diffusely enlarged thyroid with a peripheral thick rind of enhancing tissue (arrows). Results of histopathologic analysis confirmed the diagnosis of Reidel thyroiditis. **(b)** Axial postcontrast T1-weighted MR image shows a sausage-shaped pancreas with a thick hypoenhancing capsule (arrows), consistent with AIP. Note also the dilatation of an isolated intrahepatic bile duct in the posterior right hepatic lobe (arrowhead). **(c)** Axial postcontrast T1-weighted MR image depicts a peripherally enhancing, heterogeneous left adrenal mass (arrow), which proved to be an inflammatory pseudotumor at surgical excision. **(d)** MIP image from a 3D RARE MR cholangiopancreatographic study performed 4½ years later shows extensive progression of IgG4-associated cholangitis with interval development of multiple strictures involving the extra- and intrahepatic bile ducts (arrowheads). **(e)** Axial contrast-enhanced CT image demonstrates an ill-defined retroperitoneal mass with soft-tissue attenuation that partially encases the abdominal aorta (white arrowheads) and completely encases the inferior mesenteric artery (black arrowhead), findings that are consistent with retroperitoneal fibrosis.

ing the strictures (Fig 10) (39). IgG4-related sclerosing cholangitis can mimic other disease entities such as PSC, cholangiocarcinoma, pancreatic adenocarcinoma, ischemic biliary strictures, or

AIDS cholangiopathy. Unlike in PSC, multifocal strictures in IgG4-related sclerosing cholangitis are long and continuous and are associated with pre-stenotic dilatation. An elevated serum IgG4 level

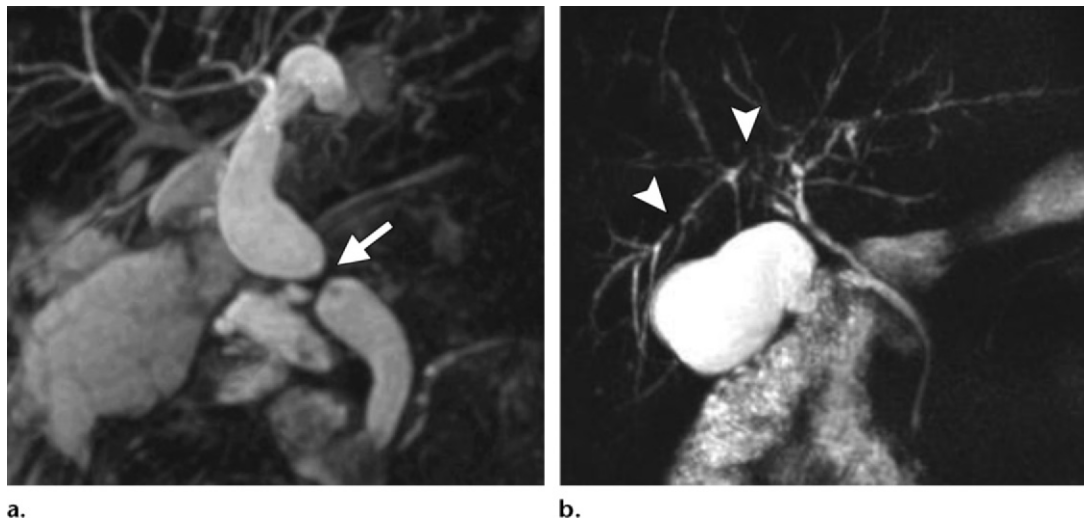


Figure 11. Biliary strictures following liver transplantation. **(a)** MR cholangiopancreatographic image obtained in a 57-year-old man who had undergone orthotopic liver transplantation 3 weeks earlier shows severe narrowing of the biliary duct–duct anastomosis (arrow), a finding that is consistent with an anastomotic stricture. **(b)** MR cholangiopancreatographic image obtained in a 39-year-old man who had recently undergone liver transplantation shows multiple discontinuous strictures involving the intrahepatic biliary ducts (arrowheads), findings that are consistent with ischemic cholangiopathy.

and the presence of extrabiliary IgG4 sclerosing disease (eg, involvement of the pancreas, kidneys, thyroid gland, and salivary glands) is strongly suggestive of IgG4-related sclerosing cholangitis.

AIP can be divided into type 1 (lymphoplasmacytic sclerosing pancreatitis) and type 2 (idiopathic duct centric pancreatitis) on the basis of distinct histologic findings and clinical profiles, although they are radiologically indistinguishable (40). Periductal lymphoplasmacytic infiltrate is present in both types of AIP. However, storiform fibrosis and obliterative phlebitis are prominent features of type 1 AIP, whereas type 2 AIP is characterized by granulocytic epithelial lesions. Patients with type 1 AIP have a high relapse rate, whereas those with type 2 AIP do not show relapse (40). Biliary tract involvement can be seen in up to 80% of patients with type 1 AIP (37,41,42). Focal stricture of the distal CBD is the most common abnormality (42). Kamisawa et al (43) showed that patients with serum IgG4 levels of 220 mg/dL or greater have a high prevalence of biliary tract involvement. Less commonly, IgG4-related sclerosing cholangitis may occur in the absence of AIP (about 7.5% cases in one study) (44).

Liver Transplantation

Biliary strictures may develop in 5%–15% of cadaveric liver transplants and 28%–32% of living donor liver transplants (45). On the basis of their pathophysiologic features, these strictures are divided into anastomotic and nonanastomotic types.

Anastomotic strictures develop due to (a) technical factors or (b) local ischemia or a bile leak in

the postoperative period, resulting in fibrosis and scar formation. They are usually single, short-segment entities that are localized to the anastomosis. Anastomotic strictures can occur with either choledochocholedochal or biliary-enteric anastomosis and are more common with Roux-en-Y reconstruction (46). MR cholangiopancreatography is equivalent to ERCP in the identification and quantification of biliary strictures and can be used as the only imaging modality in these patients (47,48). MR cholangiopancreatography shows a short-segment stricture at the site of anastomosis with possible proximal biliary dilatation (Fig 11a) (49,50).

Nonanastomotic strictures develop secondary to ischemic or immunologic causes and may lead to graft loss (45,51). These strictures are usually multiple and involve long segments, and they may develop within the liver or proximal to the anastomotic site. Ischemia may be macroangiopathic (hepatic artery thrombus or stenosis) or microangiopathic (prolonged cold and warm ischemia times, donation after cardiac death, and prolonged use of vasopressin in the donor). Immunologic causes include chronic rejection, blood type incompatibility, PSC, and autoimmune hepatitis (45). MR cholangiopancreatography shows multiple discontinuous stenoses involving the intrahepatic ducts and a long-segment stricture involving the hepatic hilum and the CHD (Fig 11b) (47–49).

Recurrent Pyogenic Cholangitis

RPC, also known as “oriental cholangiohepatitis” or intrahepatic pigmented calculus disease, is

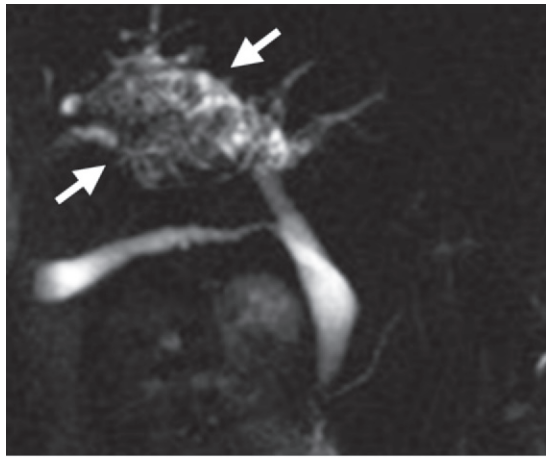
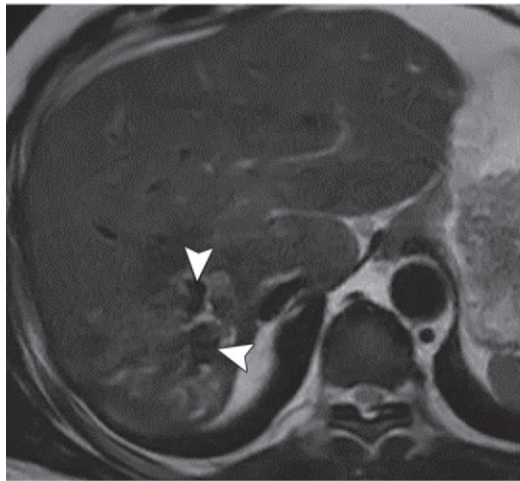
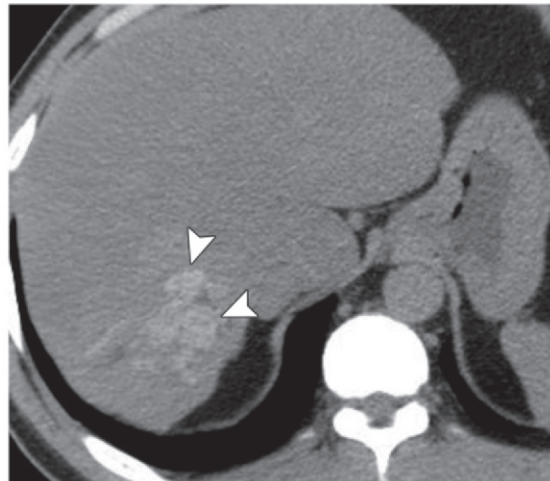


Figure 12. RPC in a 43-year-old woman. **(a)** Two-dimensional thick-slab RARE MR cholangiopancreatographic image depicts severely dilated intrahepatic bile ducts containing multiple filling defects in the right hepatic lobe (arrows). **(b)** Axial T2-weighted MR image demonstrates hypointense calculi (arrowheads) within dilated intrahepatic bile ducts of an atrophied posterior right lobe. **(c)** Axial unenhanced CT image shows hyperattenuating intraductal calculi (arrowheads).

a.



b.



c.

characterized by the presence of intrahepatic bile duct strictures and calculi (52). Clinically, RPC patients present with recurrent attacks of fever, jaundice, and abdominal pain. Although the exact cause is unknown, a strong association has been described between RPC and parasites such as *Ascariasis lumbricoides* and *Clonorchis sinensis*, as well as poor nutritional status, low socioeconomic status, and *Escherichia coli* cholangitis (52,53). Chronic inflammation and fibrosis of the bile ducts may result in multiple strictures, bile stasis, and the formation of intrahepatic calculi. MR cholangiopancreatography is superior to direct cholangiography for accurate topographic evaluation of RPC, since it depicts the entire biliary tree, in spite of multisegmental narrowing (54). **MR cholangiopancreatographic findings of RPC include intra- or extrahepatic bile duct stones, multiple intrahepatic biliary strictures, short-segment focal extrahepatic bile duct stricture, localized dilatation of lobar or segmental bile ducts with a predilection for the lateral segment of the left lobe and the posterior segment of the right lobe, bile duct wall thickening, abrupt tapering, and**

decreased arborization of the intrahepatic ducts (Fig 12) (52,53,55,56). The intraductal calculi in RPC are pigmented stones and are well visualized on T1-weighted MR images due to their hyperintensity (32). MR cholangiopancreatography has been shown to be superior in the assessment of the extent of intrahepatic stones in RPC and helps in treatment planning (57). Cholangiocarcinoma may develop in up to 5% of RPC patients; atrophied segments and hepatic segments with a high stone burden put patients at risk (58).

Mirizzi Syndrome

The term *Mirizzi syndrome* refers to stenosis and obstruction of the CHD caused by extrinsic compression from a gallstone impacted in the Hartmann pouch, which is an outpouching of the gallbladder wall either at the junction of the cystic duct and the gallbladder neck or in the cystic duct. A long cystic duct coursing parallel to the CHD and low insertion of the cystic duct into the CBD are predisposing factors in the development of Mirizzi syndrome (53,59). CHD stricture may be due to simple compression or

chronic inflammation, scar formation, or fistulization of the cystic duct to the CHD. Csendes et al (60) classified Mirizzi syndrome into four types based on the presence of fistula. Type 1 represents stricture due to external compression alone, whereas types 2–4 represent various degrees of fistulization, with an increasing defect in the CBD wall: Type 2 stricture affects less than 33% of the bile duct circumference; type 3, 33%–66%; and type 4, more than 66%. This classification is useful in guiding surgical management (59,60). Typical MR cholangiopancreatographic features of Mirizzi syndrome include cholelithiasis, a stone in the cystic duct, focal stricture of the CHD, dilatation of the intrahepatic bile ducts and proximal CHD, and a normal-caliber distal CBD (Fig 13) (53,61,62). In their study, Yun et al (63) showed that MR cholangiopancreatography with CT increases diagnostic accuracy for Mirizzi syndrome compared with CT alone by demonstrating cholelithiasis, choledocholithiasis, stenosis, and anatomic variants of the bile ducts.

AIDS Cholangiopathy

AIDS cholangiopathy is a form of secondary sclerosing cholangitis that occurs in AIDS patients with a CD4 count of less than 100/mm³ (64). Chronic inflammation of the biliary tract by opportunistic pathogens such as *Cryptosporidium parvum* and cytomegalovirus is responsible for multifocal biliary strictures in the majority of patients. Other potential causative agents include *Mycobacterium avium* complex, *Microsporidia* species, and herpes simplex virus (64). However, no pathogen is identified in up to 50% of patients (64). Clinically, patients present with elevated levels of cholestatic enzymes (eg, alkaline phosphatase and γ glutamyl transferase) and right upper quadrant pain; however, jaundice is rare, since biliary obstruction is often incomplete (64).

MR cholangiopancreatographic findings of AIDS cholangiopathy include multiple intra- and extrahepatic biliary strictures with associated dilatation simulating PSC, papillary stenosis with a dilated CBD, and an isolated intermediate- to long-segment (1–2-cm) extrahepatic bile duct stricture (Fig 14) (65,66). Other MR imaging findings include acalculous cholecystitis as well as wall thickening and enhancement of the bile ducts (66).

Sphincter of Oddi Dysfunction

SOD is due to abnormal contractility, spasm, or obstruction of the sphincter of Oddi, causing pancreaticobiliary type pain, cholestasis, or recurrent attacks of acute pancreatitis (67). SOD may be due to true stenosis or functional obstruction. It is a diagnosis of exclusion and is classified

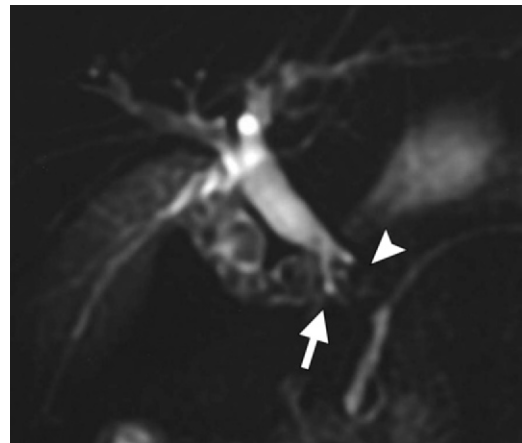


Figure 13. Mirizzi syndrome in a 47-year-old man. Two-dimensional thick-slab RARE MR cholangiopancreatographic image shows multiple calculi within the gallbladder neck and cystic duct (arrow) compressing and narrowing the CBD (arrowhead), resulting in upstream biliary dilatation, consistent with Mirizzi syndrome.



Figure 14. AIDS cholangiopathy in a 33-year-old man. Source image from a 3D RARE MR cholangiopancreatographic study shows papillary stenosis (arrow) with marked dilatation of the CBD (arrowhead) and mild prominence of the pancreatic duct, findings that are consistent with AIDS cholangiopathy.

into three biliary types (types I–III) and three pancreatic types (types I–III) based on the presence of pancreatic or biliary type pain, elevated hepatic or pancreatic enzyme levels, and dilatation of the CBD or pancreatic duct (68,69). Type I is characterized by pancreatic or biliary type pain with both an elevated enzyme level and duct dilatation; type II, by pain with either an elevated enzyme level or duct dilatation; and type III, by pain with neither an elevated enzyme level nor duct dilatation. SOD is commonly seen in patients with postcholecystectomy syndrome (persistent abdominal pain after cholecystectomy)



Figure 15. Manometrically proved SOD in a 49-year-old man. MIP image from a 3D RARE MR cholangiopancreatographic study shows moderate extrahepatic and mild intrahepatic bile duct dilatation (arrows).

and recurrent idiopathic pancreatitis, most of whom are 20–50 years old (70). A basal sphincter pressure of 40 mm Hg or greater is considered to be diagnostic for SOD (71). Endoscopic sphincter manometry is the standard test for the diagnosis of SOD; however, it is invasive, difficult to perform, and has limited availability (67,70,72). In clinically suspected cases of SOD, MR cholangiopancreatographic findings may include focal stenosis of the sphincter of Oddi, which manifests as a smoothly tapered stricture of the distal CBD and a dilated extrahepatic bile duct (usually >12 mm) with mild or no dilatation of the intrahepatic bile ducts or main pancreatic duct (MPD) (Fig 15) (67). Although a transient and minimal increase in pancreatic duct diameter is a normal finding at secretin-stimulated MR cholangiopancreatography, an increase in diameter of more than 1 mm or prolonged dilatation (>3 mm at 10 minutes) is helpful in identifying patients with suspected SOD who can benefit from intervention, especially those with type II SOD (67,73). SOD patients with evidence of inflammatory stenosis of the sphincter of Oddi at MR cholangiopancreatography can be treated successfully with endoscopic sphincterotomy.

Malignant Biliary Strictures

Cholangiocarcinoma

Cholangiocarcinoma is a malignant neoplasm that arises from both intra- and extrahepatic bile duct epithelium. Most cholangiocarcinomas are adenocarcinomas with a characteristic profuse fibrous stroma (74). On the basis of their anatomic location, cholangiocarcinomas can be classified as intrahepatic (peripheral), perihilar, or extra-

hepatic. The Liver Cancer Study Group of Japan categorized cholangiocarcinomas into mass-forming, periductal infiltrating, and intraductal growth types on the basis of morphologic features and growth patterns (75). The common risk factors for the development of cholangiocarcinomas include infection with liver flukes (*Opisthorchis viverrini* and *Clonorchis sinensis*), PSC, hepatolithiasis due to RPC, and pancreaticobiliary ductal anomalies (choledochal cyst and anomalous pancreaticobiliary junction), with chronic biliary inflammation being the common feature shared by all causes (74).

Cross-sectional imaging plays an important role in the diagnosis of cholangiocarcinoma and the assessment of resectability (76). Contrast-enhanced MR imaging with MR cholangiopancreatography is particularly useful in the evaluation of cholangiocarcinoma due to its high soft-tissue contrast resolution and its capacity to help accurately assess the extent of peripheral ductal involvement (76,77). Cholangiocarcinoma tends to show moderate peripheral enhancement followed by progressive centripetal enhancement (77). At MR imaging, periductal infiltrating and intraductal growth type cholangiocarcinomas appear as single or multifocal biliary strictures, focal or diffuse ductal thickening with or without contrast enhancement, and intraductal polypoid growth (Fig 16) (78). These findings are nonspecific and may mimic a wide spectrum of inflammatory and neoplastic conditions involving the bile ducts (53). MR imaging–MR cholangiopancreatographic findings that can help differentiate cholangiocarcinoma from other benign bile duct strictures will be discussed later.

Pancreatic Adenocarcinoma

Adenocarcinoma is the most common malignant neoplasm of the pancreas in adults. About 70% of tumors occur in the head, neck, and uncinate process and usually manifest with obstructive jaundice secondary to stricture of the intrapancreatic portion of the CBD (79). Multidetector CT and MR imaging are equally effective in tumor detection (sensitivity of 91% and 84%, respectively) and assessment of tumor resectability (sensitivity of 82% and 81%, respectively) (80). However, MR imaging is commonly used as a “problem-solving” tool in suspected non-contour-deforming pancreatic masses at multidetector CT, small masses (<2 cm), and patients with inconclusive CT findings (81). In addition, hepatic, peritoneal, and omental metastases can be detected much more easily at MR imaging than at CT. In one study, contrast-enhanced MR imaging demonstrated an accuracy of approximately 94% for vascular involvement (82). Pancreatic

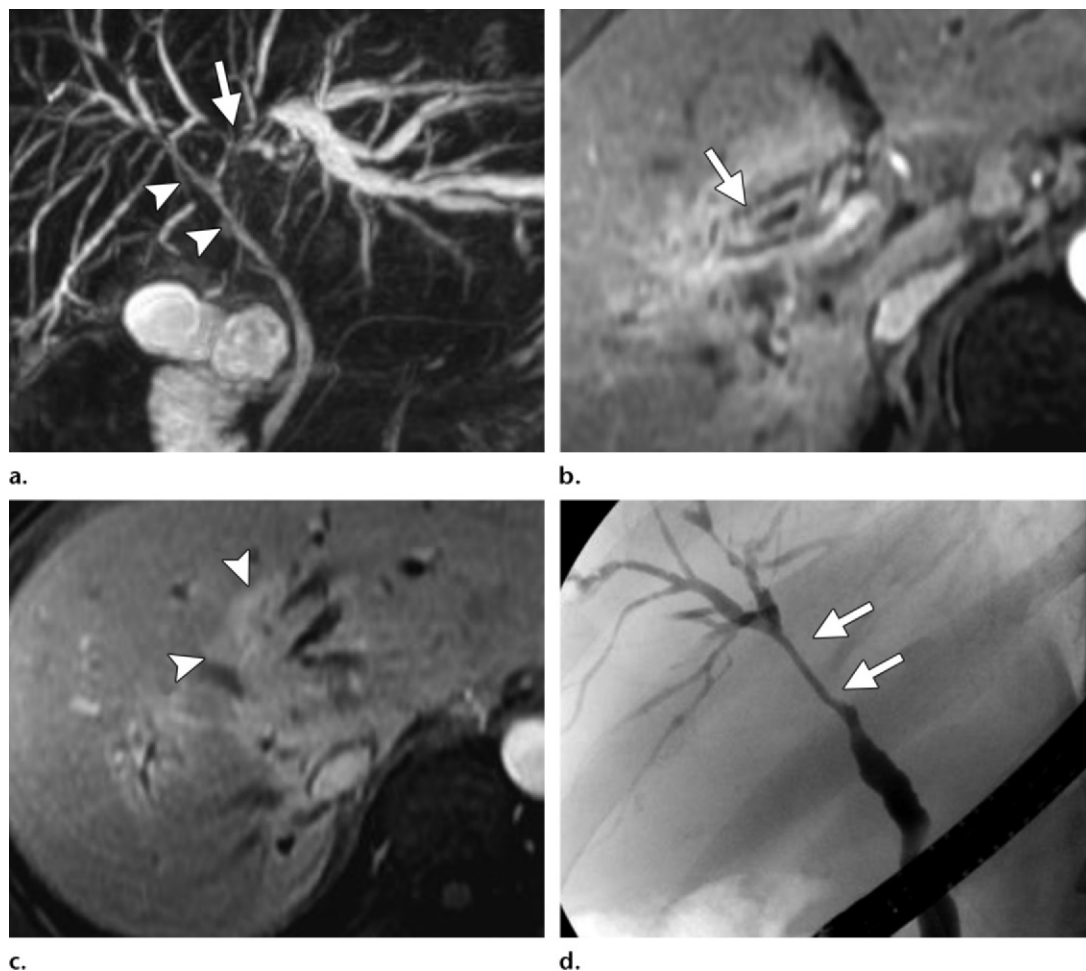


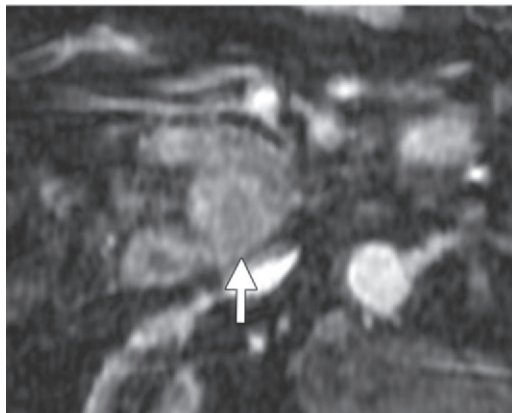
Figure 16. Cholangiocarcinoma in a 60-year-old man with known PSC who presented with a 2-month history of a rapidly increasing serum bilirubin level. **(a)** MIP image from a 3D RARE MR cholangiopancreatographic study shows severe narrowing of the left hepatic duct (arrow) and, to a lesser extent, narrowing of the RHD and proximal CHD (arrowheads). **(b, c)** Axial contrast-enhanced MR images obtained at different levels of the liver show circumferential wall thickening and enhancement of the RHD (arrow in **b**) and an enhancing mass occluding the left hepatic duct (arrowheads in **c**), with moderate dilatation of the left lobar intrahepatic bile ducts. **(d)** ERCP image demonstrates a long-segment stricture of the RHD (arrows) without significant upstream biliary dilatation. The left hepatic duct was not opacified with contrast material, likely owing to severe narrowing. Biopsy of the RHD using the Spyglass Spyscope system (Boston Scientific, Natick, Mass) showed an invasive, moderately differentiated cholangiocarcinoma.

adenocarcinoma is hypointense on frequency-selective fat-suppressed T1-weighted images and iso- to slightly hyperintense on T2-weighted images. Typically, four sets of fat-saturated T1-weighted images are obtained, at 20 seconds (arterial phase), 50 seconds (pancreatic phase), 90 seconds (portal venous phase), and 120 seconds (delayed phase) after the administration of gadolinium-based contrast material (83). The mass enhances less than the background pancreatic parenchyma on arterial and pancreatic phase images, and then shows progressive enhancement in the portal venous and delayed phases (81,84). MR imaging findings of the mass are indicative of abundant fibrous stroma within the pancreatic adenocarcinoma. MR cholangiopancreatography

shows abrupt termination of the CBD and MPD at the level of the mass in the pancreas with upstream ductal dilatation (83,84). This MR cholangiopancreatographic appearance is often described as the “double duct sign,” which occurs with narrowing of the intrapancreatic CBD and the MPD secondary to contiguous obstruction or encasement by a mass of the pancreatic head (Fig 17) (85). Although highly suggestive, the double duct sign is not diagnostic for pancreatic head carcinoma, since it can be seen in other malignancies such as ampullary cancer, distal CBD cholangiocarcinoma, and duodenal carcinoma or lymphoma, and in benign entities such as chronic pancreatitis and ampullary stenosis (85). Although CT and MR imaging are very helpful



a.



b.

Figure 17. Pancreatic adenocarcinoma in a 77-year-old man. **(a)** MIP image from a 3D RARE MR cholangiopancreatographic study shows a short-segment stricture of the intrapancreatic portion of the CBD (arrow) with upstream biliary dilatation as well as several cystic foci communicating with the MPD (arrowheads), findings that are consistent with multifocal branch-duct type intraductal papillary mucinous tumor. **(b)** Axial postcontrast MR image shows a hypoenhancing focal mass in the pancreatic head (arrow), consistent with adenocarcinoma.

in assessing local tumor invasion and surgical resectability, positron emission tomography can be useful as a problem-solving technique and aids in differentiating benign from malignant lesions, detecting unsuspected metastases, and differentiating residual or recurrent tumor from postsurgical scar tissue (86).

Ampullary and Periampullary Carcinomas

Ampullary carcinoma is defined as carcinoma arising in the ampullary complex distal to the confluence of the pancreatic duct and CBD. Ma-

lignant tumors arising within 2 cm of the major duodenal papilla can be categorized as periampullary carcinomas and include carcinoma of the ampulla of Vater, distal CBD, head and uncinate process of the pancreas, and periampullary portion of the duodenum (87). These malignancies show varied tumor biologic features that result in different long-term outcomes; accurate differentiation among these entities is critical for treatment planning and may help predict prognosis (87). Although patients with ampullary or duodenal carcinoma have better 5-year survival rates than do those with bile duct or pancreatic carcinoma (87), it is important to exclude a benign cause for ampullary obstruction before considering various periampullary carcinomas. **Identification of an ampullary mass, papillary bulging, irregular asymmetric luminal narrowing of the distal CBD, and diffuse upstream intra- and extrahepatic biliary dilatation are signs of malignant ampullary obstruction, whereas smooth symmetric luminal narrowing of the CBD and central biliary dilatation without an ampullary mass or papillary bulging are expected with a benign obstruction** (88). Although difficult, analysis of MR imaging and MR cholangiopancreatographic findings in terms of mass location and shape and pattern of biliary and pancreatic duct dilatation is extremely helpful in differentiating among various periampullary malignancies (89).

Ampullary carcinoma is a rare malignancy arising from the ampulla of Vater that may appear at MR imaging as a small nodular mass, periductal thickening, or bulging of duodenal papillae (87). If identified, the mass is isointense relative to the adjacent duodenal wall on T1-weighted images and shows variable signal intensity on T2-weighted images. At arterial phase imaging, the mass is hypointense relative to the surrounding duodenum and shows delayed contrast enhancement (Fig 18) (89). MR cholangiopancreatography may show marked abrupt dilatation of the distal CBD or the pancreatic duct without signs of pancreatitis or an obvious pancreatic mass or stone. Distal CBD malignancy may manifest as irregular ductal wall thickening with luminal obliteration or as an intraductal polypoid mass (87). A normal pancreatic duct is seen in most cases, unless there is tumor invasion into the ampullary portion or direct involvement of the pancreatic duct through the pancreatic parenchyma. Periampullary duodenal adenocarcinoma may manifest at MR imaging as a polypoid mass, fungating mass, or eccentric duodenal wall thickening (Fig 19a), with associated dilatation of the pancreatic duct and CBD (Fig 19b) (87). This dilatation is modest or absent in duodenal carcinoma when the periampullary portion is spared.

Teaching Point

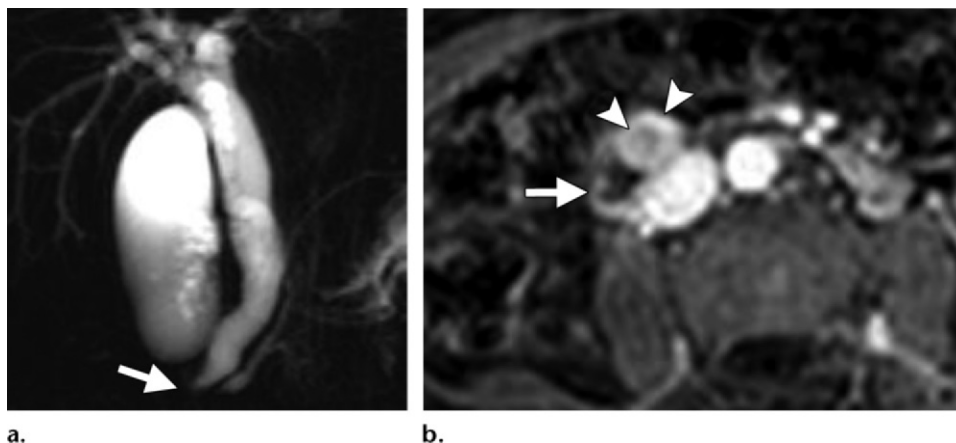


Figure 18. Ampullary adenocarcinoma in a 62-year-old woman. **(a)** Two-dimensional thick-slab RARE MR cholangiopancreatographic image shows abrupt narrowing of the distal CBD at the level of the ampulla (arrow), along with marked dilatation of the CBD and mild prominence of the MPD. **(b)** Axial postcontrast MR image shows an enhancing ampullary mass (arrowheads) protruding into the lumen of the second portion of the duodenum (arrow). The mass proved to be an ampullary adenocarcinoma at surgical resection.

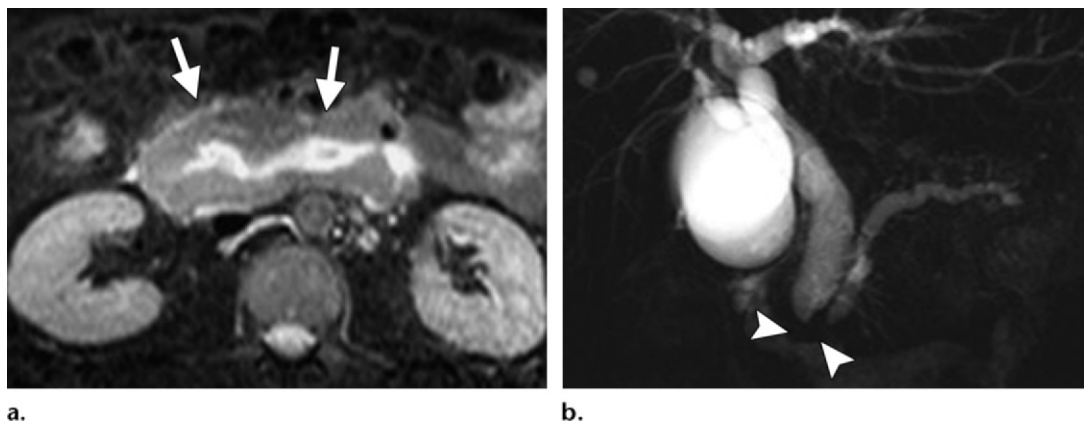


Figure 19. Duodenal adenocarcinoma in a 68-year-old woman. **(a)** Axial T2-weighted MR image demonstrates circumferential nodular thickening of the second and third portions of the duodenum (arrows). **(b)** Two-dimensional thick-slab RARE MR cholangiopancreatographic image depicts abrupt focal narrowing of the distal CBD and pancreatic duct at the ampulla (arrowheads) with moderate dilatation of the upstream biliary tree and pancreatic duct. Duodenal adenocarcinoma was diagnosed at endoscopy-guided biopsy.

In addition, lymphoma of the second portion of the duodenum involving the periampullary region may also result in strictures of the distal CBD with upstream biliary dilatation (Fig 20).

Miscellaneous and Rare Causes

Biliary inflammatory pseudotumor is an extremely rare and poorly understood entity that manifests as an infiltrative lesion mimicking hilar or intrahepatic cholangiocarcinoma and is characterized histologically by an admixture of fibrovascular tissue and a cellular infiltrate of plasma cells, eosinophils, and histiocytes (90). Follicular cholangitis is another extremely rare disease entity that mimics hilar cholangiocarcinoma and is characterized histologically by numerous lym-

phoid follicles around hilar or perihilar bile ducts (91). At MR cholangiopancreatography, both biliary inflammatory pseudotumor and follicular cholangitis can mimic hilar cholangiocarcinoma when they cause a hilar stricture with intrahepatic biliary ductal dilatation. When intrahepatic bile ducts are involved, the MR imaging and MR cholangiopancreatographic findings mimic peripheral cholangiocarcinoma (Fig 21). Hepatocellular carcinoma and gallbladder carcinoma may cause biliary strictures, either by direct extension of the tumor to the porta hepatis or by compression of the extrahepatic bile ducts by enlarged porta hepatis lymph nodes (92). Gallbladder carcinoma involving the body and neck of the gallbladder may extend up to the porta hepatis and

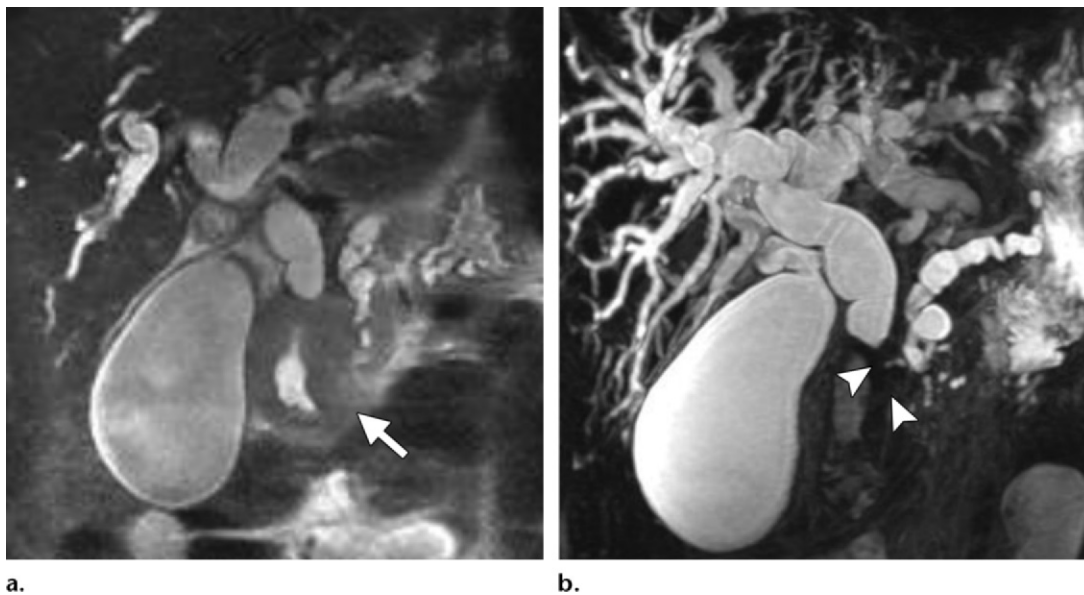


Figure 20. Periamпуляр lymphoma in a 55-year-old man. **(a)** Coronal half-Fourier acquisition single-shot turbo spin-echo image shows circumferential wall thickening of the second portion of the duodenum (arrow) with marked biliary and pancreatic ductal dilatation. **(b)** MIP image from a 3D RARE MR cholangiopancreatographic study demonstrates strictures of the pancreatic duct and CBD near the ampulla (arrowheads) with marked upstream dilatation. The diagnosis of non-Hodgkin lymphoma was confirmed at histopathologic analysis.

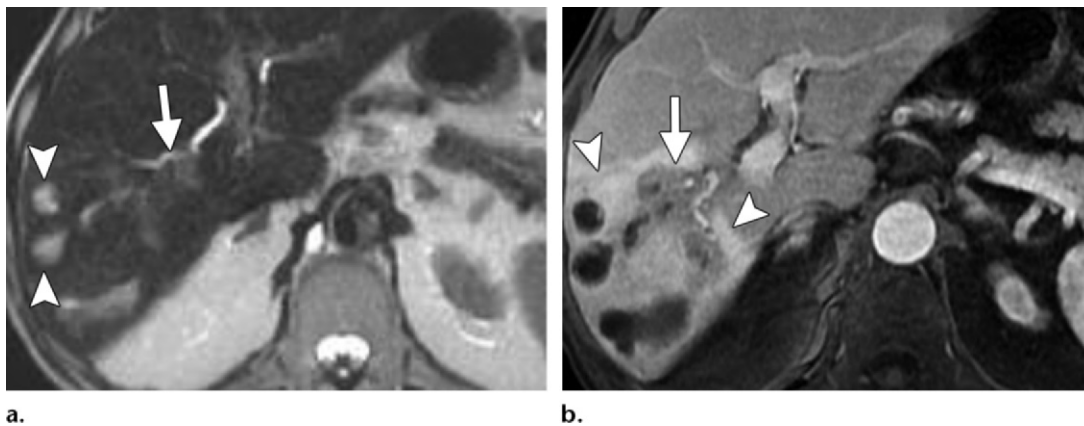


Figure 21. Biliary inflammatory pseudotumor in an 83-year-old man. **(a)** Axial T2-weighted MR image shows a masslike area with faint hyperintensity in the right hepatic lobe (arrow) with upstream biliary ductal dilatation (arrowheads). **(b)** Axial postcontrast MR image shows an infiltrative masslike area (arrow) encasing the RHD, with marked upstream dilatation of the intrahepatic bile ducts within an atrophic hyperenhancing right hepatic lobe (arrowheads). Histopathologic analysis revealed severe lymphoplasmacytic and neutrophilic infiltration without evidence of malignancy, findings that are consistent with biliary inflammatory pseudotumor.

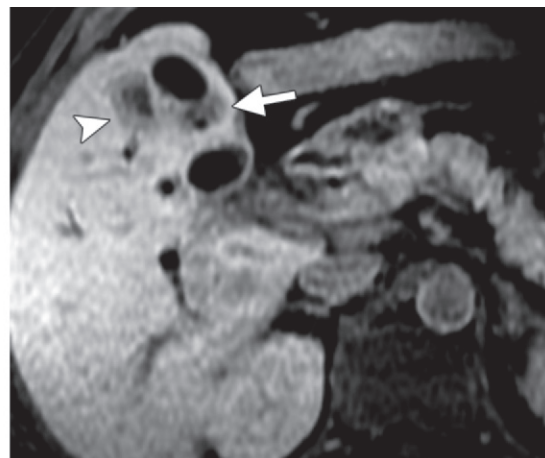
cause CHD stricture (Fig 22). Biliary metastases are very rare and may cause strictures mimicking cholangiocarcinoma. They are commonly from primary cancers of the lung, breast, gallbladder, and colon. Biliary involvement by metastatic melanoma and lymphomatous infiltration has also been documented (53). Among these primary cancers, colon cancer has a greater predilection for the bile ducts due to its proclivity to spread along epithelial surfaces (53). Periportal

and peripancreatic lymphadenopathy may cause CHD-CBD strictures secondary to compression (92). Malignancies of the gallbladder, pancreas, stomach, and colon are the usual culprits (92).

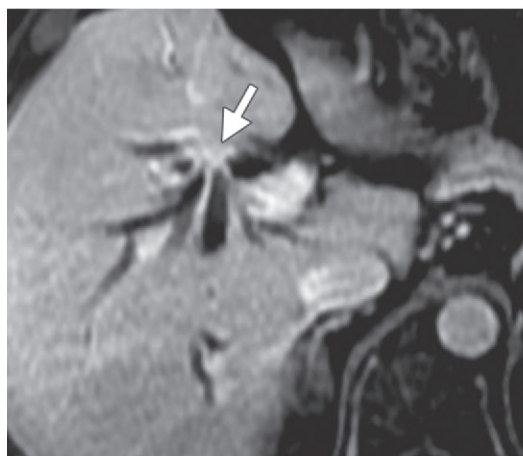
Differentiation of Malignant from Benign Biliary Strictures

Differentiation of malignant from benign bile duct strictures is critical for optimal patient management. ERCP is a crucial tool in the workup of

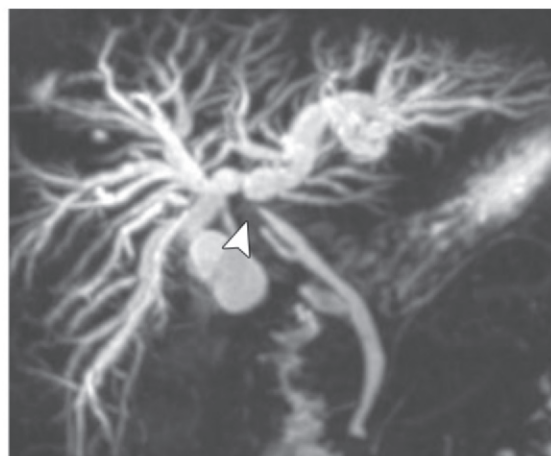
Figure 22. Gallbladder adenocarcinoma causing biliary obstruction in a 58-year-old man. **(a)** Axial postcontrast delayed phase MR image shows a faintly enhancing mass (arrow) involving the gallbladder with extension into the adjacent liver parenchyma (arrowhead). **(b)** Axial contrast-enhanced portal venous phase MR image shows a small enhancing mass at the hepatic hilum (arrow) that is contiguous with the gallbladder mass, with associated moderate intrahepatic biliary ductal dilatation. **(c)** MIP image from a 3D RARE MR cholangiopancreatographic study shows moderate bilobar intrahepatic biliary ductal dilatation secondary to a stricture of the proximal CHD and hepatic ductal confluence (arrowhead).



a.



b.



c.

a patient with suspected biliary obstruction because it yields high-spatial-resolution images; allows tissue biopsy, thereby aiding in establishing the diagnosis; and has therapeutic applications. However, ERCP is an invasive procedure that requires an intravenously administered sedative and ionizing radiation, and it is relatively time consuming. In addition, ERCP is expensive, may be technically unsuccessful in about 4% of patients, can result in incomplete evaluation in patients with high-grade strictures due to nonvisualization of upstream ducts, and is associated with a complication rate of up to 7% and a mortality rate of 0.1%–0.9% (93,94). The biochemical and imaging predictors of malignant biliary strictures have been investigated in many clinical studies (12,95–97). Patients with a serum bilirubin level of over 8.4 mg/dL and a CA 19–9 level of over 100 U/L are more likely to have malignant strictures (95,96). In addition, greater patient age, proximal biliary dilatation, and higher levels of bilirubin, alkaline phosphatase, and transaminases are associated with malignancy (95).

Visualization of biliary ductal morphology with MR imaging—MR cholangiopancreatogra-

phy is comparable to that with ERCP (98). Additional advantages include good patient tolerance, no associated mortality, 3D imaging, the ability to depict ducts upstream to high-grade strictures, and usefulness in planning percutaneous biliary interventions (99). However, MR imaging may lead to overestimation of length and grade of biliary stricture, and in patients with severe claustrophobia or (for example) intracranial aneurysmal clips, cardiac pacemakers, or cochlear implants, imaging cannot be performed and a tissue specimen cannot be obtained for definitive diagnosis. Unenhanced and contrast-enhanced MR imaging with MR cholangiopancreatography is extremely helpful in the evaluation of the narrowed bile duct segment and may suggest findings that are specific for a malignant cause (Table 3). In their study, Park et al (97) concluded that MR cholangiopancreatography is comparable to ERCP in differentiating extrahepatic bile duct cholangiocarcinoma from a benign stricture and showed that a lengthy narrowed segment with irregular margins and asymmetric narrowing is suggestive of malignancy. Kim et al (12) showed that a narrowed segment with the following MR imaging

Table 3: MR Imaging–MR Cholangiopancreatographic Findings That Suggest Malignant Biliary Strictures

Wall thickening
Long-segment involvement
Asymmetry
Indistinct outer margin
Luminal irregularity
Hyperenhancement relative to liver parenchyma during portal venous phase

Sources.—References 12 and 97.

features is more likely to be malignant: hyperenhancement relative to the liver during the portal venous phase, length of over 12 mm, wall thickness greater than 3 mm, indistinct outer margin, luminal irregularity, and asymmetry.

Conclusion

There is a wide spectrum of causes for biliary strictures in adult patients, including both benign and malignant conditions. Contrast-enhanced MR imaging with MR cholangiopancreatography is very useful in the evaluation of the bile ducts in patients with obstructive jaundice. Although biopsy is necessary for distinguishing malignant from benign strictures, certain MR imaging findings of the narrowed segment may favor a malignant cause.

References

- Darge K, Anupindi SA, Jaramillo D. MR imaging of the abdomen and pelvis in infants, children, and adolescents. *Radiology* 2011;261(1):12–29.
- Shanmugam V, Beattie GC, Yule SR, Reid W, Loudon MA. Is magnetic resonance cholangiopancreatography the new gold standard in biliary imaging? *Br J Radiol* 2005;78(934):888–893.
- Afdhal NH. Diseases of the gallbladder and bile ducts. In: Goldman L, Schafer AI, eds. *Cecil medicine*. 24th ed. Philadelphia, Pa: Saunders Elsevier, 2011.
- Cursio R, Gugenheim J. Ischemia-reperfusion injury and ischemic-type biliary lesions following liver transplantation. *J Transplant* 2012;2012:164329.
- Lee WJ, Lim HK, Jang KM, et al. Radiologic spectrum of cholangiocarcinoma: emphasis on unusual manifestations and differential diagnoses. *RadioGraphics* 2001;21(Spec No):S97–S116.
- Wallner BK, Schumacher KA, Weidenmaier W, Friedrich JM. Dilated biliary tract: evaluation with MR cholangiography with a T2-weighted contrast-enhanced fast sequence. *Radiology* 1991;181(3):805–808.
- Yeh BM, Liu PS, Soto JA, Corvera CA, Hussain HK. MR imaging and CT of the biliary tract. *RadioGraphics* 2009;29(6):1669–1688.
- Choi JY, Lee JM, Lee JY, et al. Navigator-triggered isotropic three-dimensional magnetic resonance cholangiopancreatography in the diagnosis of malignant biliary obstructions: comparison with direct cholangiography. *J Magn Reson Imaging* 2008;27(1):94–101.
- Vitellas KM, Keogan MT, Spritzer CE, Nelson RC. MR cholangiopancreatography of bile and pancreatic duct abnormalities with emphasis on the single-shot fast spin-echo technique. *RadioGraphics* 2000;20(4):939–957.
- Sodickson A, Mortelet KJ, Barish MA, Zou KH, Thibodeau S, Tempny CM. Three-dimensional fast-recovery fast spin-echo MRCP: comparison with two-dimensional single-shot fast spin-echo techniques. *Radiology* 2006;238(2):549–559.
- Sahni VA, Mortelet KJ. Magnetic resonance cholangiopancreatography: current use and future applications. *Clin Gastroenterol Hepatol* 2008;6(9):967–977.
- Kim JY, Lee JM, Han JK, et al. Contrast-enhanced MRI combined with MR cholangiopancreatography for the evaluation of patients with biliary strictures: differentiation of malignant from benign bile duct strictures. *J Magn Reson Imaging* 2007;26(2):304–312.
- Lee NK, Kim S, Lee JW, et al. Biliary MR imaging with Gd-EOB-DTPA and its clinical applications. *RadioGraphics* 2009;29(6):1707–1724.
- Irie H, Honda H, Kuroiwa T, et al. Pitfalls in MR cholangiopancreatographic interpretation. *RadioGraphics* 2001;21(1):23–37.
- Kondo H, Kanematsu M, Shiratori Y, Moriwaki H, Hoshi H. Potential pitfall of MR cholangiopancreatography: right hepatic arterial impression of the common hepatic duct. *J Comput Assist Tomogr* 1999;23(1):60–62.
- Moser AJ. Benign biliary strictures. *Curr Treat Options Gastroenterol* 2001;4(5):377–387.
- Jabłońska B, Lampe P. Iatrogenic bile duct injuries: etiology, diagnosis and management. *World J Gastroenterol* 2009;15(33):4097–4104.
- Khalid TR, Casillas VJ, Montalvo BM, Centeno R, Levi JU. Using MR cholangiopancreatography to evaluate iatrogenic bile duct injury. *AJR Am J Roentgenol* 2001;177(6):1347–1352.
- Girometti R, Brondani G, Cereser L, et al. Post-cholecystectomy syndrome: spectrum of biliary findings at magnetic resonance cholangiopancreatography. *Br J Radiol* 2010;83(988):351–361.
- Karvonen J, Gullichsen R, Laine S, Salminen P, Grönroos JM. Bile duct injuries during laparoscopic cholecystectomy: primary and long-term results from a single institution. *Surg Endosc* 2007;21(7):1069–1073.
- Ward J, Sheridan MB, Guthrie JA, et al. Bile duct strictures after hepatobiliary surgery: assessment with MR cholangiography. *Radiology* 2004;231(1):101–108.

22. Chaudhary A, Negi SS, Puri SK, Narang P. Comparison of magnetic resonance cholangiography and percutaneous transhepatic cholangiography in the evaluation of bile duct strictures after cholecystectomy. *Br J Surg* 2002;89(4):433–436.
23. Hoeffel C, Azizi L, Lewin M, et al. Normal and pathologic features of the postoperative biliary tract at 3D MR cholangiopancreatography and MR imaging. *RadioGraphics* 2006;26(6):1603–1620.
24. Abdallah AA, Krige JE, Bornman PC. Biliary tract obstruction in chronic pancreatitis. *HPB (Oxford)* 2007;9(6):421–428.
25. Hakimé A, Giraud M, Vullierme MP, Vilgrain V. MR imaging of the pancreas [in French]. *J Radiol* 2007;88(1 pt 1):11–25.
26. Robinson PJ, Sheridan MB. Pancreatitis: computed tomography and magnetic resonance imaging. *Eur Radiol* 2000;10(3):401–408.
27. Ko CW, Lee SP. Epidemiology and natural history of common bile duct stones and prediction of disease. *Gastrointest Endosc* 2002;56(6 suppl):S165–S169.
28. Williams EJ, Green J, Beekingham I, et al. Guidelines on the management of common bile duct stones (CBDS). *Gut* 2008;57(7):1004–1021.
29. Gallix BP, Régent D, Bruel JM. Use of magnetic resonance cholangiography in the diagnosis of choledocholithiasis. *Abdom Imaging* 2001;26(1):21–27.
30. Shi EC, Ham JM. Benign biliary strictures associated with chronic pancreatitis and gallstones. *Aust N Z J Surg* 1980;50(5):488–492.
31. Vitellas KM, Keogan MT, Freed KS, et al. Radiologic manifestations of sclerosing cholangitis with emphasis on MR cholangiopancreatography. *RadioGraphics* 2000;20(4):959–975.
32. Knowlton JQ, Taylor AJ, Reichelderfer M, Stang J. Imaging of biliary tract inflammation: an update. *AJR Am J Roentgenol* 2008;190(4):984–992.
33. Bader TR, Beavers KL, Semelka RC. MR imaging features of primary sclerosing cholangitis: patterns of cirrhosis in relationship to clinical severity of disease. *Radiology* 2003;226(3):675–685.
34. Ito K, Mitchell DG, Outwater EK, Blasbalg R. Primary sclerosing cholangitis: MR imaging features. *AJR Am J Roentgenol* 1999;172(6):1527–1533.
35. Walker SL, McCormick PA. Diagnosing cholangiocarcinoma in primary sclerosing cholangitis: an “evidence based radiology” review. *Abdom Imaging* 2008;33(1):14–17.
36. MacCarty RL, LaRusso NF, May GR, et al. Cholangiocarcinoma complicating primary sclerosing cholangitis: cholangiographic appearances. *Radiology* 1985;156(1):43–46.
37. Shimosegawa T, Chari ST, Frulloni L, et al. International consensus diagnostic criteria for autoimmune pancreatitis: guidelines of the International Association of Pancreatology. *Pancreas* 2011;40(3):352–358.
38. Nakazawa T, Ohara H, Sano H, Ando T, Joh T. Schematic classification of sclerosing cholangitis with autoimmune pancreatitis by cholangiography. *Pancreas* 2006;32(2):229.
39. Vlachou PA, Khalili K, Jang HJ, Fischer S, Hirschfield GM, Kim TK. IgG4-related sclerosing disease: autoimmune pancreatitis and extrapancreatic manifestations. *RadioGraphics* 2011;31(5):1379–1402.
40. Sah RP, Chari ST, Pannala R, et al. Differences in clinical profile and relapse rate of type 1 versus type 2 autoimmune pancreatitis. *Gastroenterology* 2010;139(1):140–148.
41. Bodily KD, Takahashi N, Fletcher JG, et al. Autoimmune pancreatitis: pancreatic and extrapancreatic imaging findings. *AJR Am J Roentgenol* 2009;192(2):431–437.
42. Kamisawa T, Egawa N, Nakajima H, Tsuruta K, Okamoto A. Extrapancreatic lesions in autoimmune pancreatitis. *J Clin Gastroenterol* 2005;39(10):904–907.
43. Kamisawa T, Imai M, Egawa N, Tsuruta K, Okamoto A. Serum IgG4 levels and extrapancreatic lesions in autoimmune pancreatitis. *Eur J Gastroenterol Hepatol* 2008;20(12):1167–1170.
44. Ghazale A, Chari ST, Zhang L, et al. Immunoglobulin G4-associated cholangitis: clinical profile and response to therapy. *Gastroenterology* 2008;134(3):706–715.
45. Ayoub WS, Esquivel CO, Martin P. Biliary complications following liver transplantation. *Dig Dis Sci* 2010;55(6):1540–1546.
46. Pascher A, Neuhaus P. Biliary complications after deceased-donor orthotopic liver transplantation. *J Hepatobiliary Pancreat Surg* 2006;13(6):487–496.
47. Kitazono MT, Qayyum A, Yeh BM, Chard PS, Ostroff JW, Coakley FV. Magnetic resonance cholangiography of biliary strictures after liver transplantation: a prospective double-blind study. *J Magn Reson Imaging* 2007;25(6):1168–1173.
48. Valls C, Alba E, Cruz M, et al. Biliary complications after liver transplantation: diagnosis with MR cholangiopancreatography. *AJR Am J Roentgenol* 2005;184(3):812–820.
49. Novellas S, Caramella T, Fournol M, Gugenheim J, Chevallier P. MR cholangiopancreatography features of the biliary tree after liver transplantation. *AJR Am J Roentgenol* 2008;191(1):221–227.
50. Singh AK, Nachiappan AC, Verma HA, et al. Postoperative imaging in liver transplantation: what radiologists should know. *RadioGraphics* 2010;30(2):339–351.
51. Guichelaar MM, Benson JT, Malinchoc M, Krom RA, Wiesner RH, Charlton MR. Risk factors for and clinical course of non-anastomotic biliary strictures after liver transplantation. *Am J Transplant* 2003;3(7):885–890.
52. Heffernan EJ, Geoghegan T, Munk PL, Ho SG, Harris AC. Recurrent pyogenic cholangitis: from imaging to intervention. *AJR Am J Roentgenol* 2009;192(1):W28–W35.
53. Menias CO, Surabhi VR, Prasad SR, Wang HL, Narra VR, Chintapalli KN. Mimics of cholangiocarcinoma: spectrum of disease. *RadioGraphics* 2008;28(4):1115–1129.
54. Park MS, Yu JS, Kim KW, et al. Recurrent pyogenic cholangitis: comparison between MR cholangiography and direct cholangiography. *Radiology* 2001;220(3):677–682.
55. Jain M, Agarwal A. MRCP findings in recurrent pyogenic cholangitis. *Eur J Radiol* 2008;66(1):79–83.
56. Kim MJ, Cha SW, Mitchell DG, Chung JJ, Park S, Chung JB. MR imaging findings in recurrent pyogenic cholangitis. *AJR Am J Roentgenol* 1999;173(6):1545–1549.
57. Kim TK, Kim BS, Kim JH, et al. Diagnosis of intrahepatic stones: superiority of MR cholangiopancreatography over endoscopic retrograde cholangiopancreatography. *AJR Am J Roentgenol* 2002;179(2):429–434.

58. Chen MF, Jan YY, Wang CS, et al. A reappraisal of cholangiocarcinoma in patient with hepatolithiasis. *Cancer* 1993;71(8):2461–2465.
59. Ahlawat SK, Singhania R, Al-Kawas FH. Mirizzi syndrome. *Curr Treat Options Gastroenterol* 2007;10(2):102–110.
60. Csendes A, Diaz JC, Burdiles P, Maluenda F, Nava O. Mirizzi syndrome and cholecystobiliary fistula: a unifying classification. *Br J Surg* 1989;76(11):1139–1143.
61. Choi BW, Kim MJ, Chung JJ, Chung JB, Yoo HS, Lee JT. Radiologic findings of Mirizzi syndrome with emphasis on MRI. *Yonsei Med J* 2000;41(1):144–146.
62. Kim PN, Outwater EK, Mitchell DG. Mirizzi syndrome: evaluation by MRI imaging. *Am J Gastroenterol* 1999;94(9):2546–2550.
63. Yun EJ, Choi CS, Yoon DY, et al. Combination of magnetic resonance cholangiopancreatography and computed tomography for preoperative diagnosis of the Mirizzi syndrome. *J Comput Assist Tomogr* 2009;33(4):636–640.
64. Keaveny AP, Karasik MS. Hepatobiliary and pancreatic infections in AIDS. I. *AIDS Patient Care STDS* 1998;12(5):347–357.
65. Vermani N, Kang M, Khandelwal N, Singh P, Chawla YK. MR cholangiopancreatographic demonstration of biliary tract abnormalities in AIDS cholangiopathy: report of two cases. *Clin Radiol* 2009;64(3):335–338.
66. Bilgin M, Balci NC, Erdogan A, Momtahan AJ, Alkaade S, Rau WS. Hepatobiliary and pancreatic MRI and MRCP findings in patients with HIV infection. *AJR Am J Roentgenol* 2008;191(1):228–232.
67. Pereira SP, Gillams A, Sgouros SN, Webster GJ, Hatfield AR. Prospective comparison of secretin-stimulated magnetic resonance cholangiopancreatography with manometry in the diagnosis of sphincter of Oddi dysfunction types II and III. *Gut* 2007;56(6):809–813.
68. Geenen JE, Hogan WJ, Dodds WJ, Toouli J, Venu RP. The efficacy of endoscopic sphincterotomy after cholecystectomy in patients with sphincter-of-Oddi dysfunction. *N Engl J Med* 1989;320(2):82–87.
69. Petersen BT. Sphincter of Oddi dysfunction. II. Evidence-based review of the presentations, with “objective” pancreatic findings (types I and II) and of presumptive type III. *Gastrointest Endosc* 2004;59(6):670–687.
70. Bistriz L, Bain VG. Sphincter of Oddi dysfunction: managing the patient with chronic biliary pain. *World J Gastroenterol* 2006;12(24):3793–3802.
71. Behar J, Corazziari E, Guelrud M, Hogan W, Sherman S, Toouli J. Functional gallbladder and sphincter of oddi disorders. *Gastroenterology* 2006;130(5):1498–1509.
72. Hogan WJ, Sherman S, Pasricha P, Carr-Locke D. Sphincter of Oddi manometry. *Gastrointest Endosc* 1997;45(3):342–348.
73. Matos C, Cappeliez O, Winant C, Coppens E, Devière J, Metens T. MR imaging of the pancreas: a pictorial tour. *RadioGraphics* 2002;22(1):e2.
74. Chung YE, Kim MJ, Park YN, et al. Varying appearances of cholangiocarcinoma: radiologic-pathologic correlation. *RadioGraphics* 2009;29(3):683–700.
75. Liver Cancer Study Group of Japan. General rules for the clinical and pathological study of primary liver cancer, 2nd English edition. Tokyo, Japan: Kanehara, 2003. [The 2000 4th Japanese edition corresponds to the 2003 2nd English edition.]
76. Sainani NI, Catalano OA, Holalkere NS, Zhu AX, Hahn PF, Sahani DV. Cholangiocarcinoma: current and novel imaging techniques. *RadioGraphics* 2008;28(5):1263–1287.
77. Slattery JM, Sahani DV. What is the current state-of-the-art imaging for detection and staging of cholangiocarcinoma? *Oncologist* 2006;11(8):913–922.
78. Han JK, Choi BI, Kim AY, et al. Cholangiocarcinoma: pictorial essay of CT and cholangiographic findings. *RadioGraphics* 2002;22(1):173–187.
79. Chhibber S, Sharma AK, Kumar N, Ghumman S, Puri SK. Pancreatic tumors: prospective evaluation using MR imaging with MR cholangiography and MR angiography. *Indian J Radiol Imaging* 2006;16(4):515–521.
80. Bipat S, Phoa SS, van Delden OM, et al. Ultrasonography, computed tomography and magnetic resonance imaging for diagnosis and determining resectability of pancreatic adenocarcinoma: a meta-analysis. *J Comput Assist Tomogr* 2005;29(4):438–445.
81. Sahani DV, Shah ZK, Catalano OA, Boland GW, Bruge WR. Radiology of pancreatic adenocarcinoma: current status of imaging. *J Gastroenterol Hepatol* 2008;23(1):23–33.
82. Sironi S, De Cobelli F, Zerbi A, et al. Pancreatic adenocarcinoma: assessment of vascular invasion with high-field MR imaging and a phased-array coil. *AJR Am J Roentgenol* 1996;167(4):997–1001.
83. Miller FH, Rini NJ, Keppke AL. MRI of adenocarcinoma of the pancreas. *AJR Am J Roentgenol* 2006;187(4):W365–W374.
84. Vachiranubhap B, Kim YH, Balci NC, Semelka RC. Magnetic resonance imaging of adenocarcinoma of the pancreas. *Top Magn Reson Imaging* 2009;20(1):3–9.
85. Ahualli J. The double duct sign. *Radiology* 2007;244(1):314–315.
86. Kalra MK, Maher MM, Boland GW, Saini S, Fischman AJ. Correlation of positron emission tomography and CT in evaluating pancreatic tumors: technical and clinical implications. *AJR Am J Roentgenol* 2003;181(2):387–393.
87. Kim JH, Kim MJ, Chung JJ, Lee WJ, Yoo HS, Lee JT. Differential diagnosis of periampullary carcinomas at MR imaging. *RadioGraphics* 2002;22(6):1335–1352.
88. Chung YE, Kim MJ, Kim HM, et al. Differentiation of benign and malignant ampullary obstructions on MR imaging. *Eur J Radiol* 2011;80(2):198–203.
89. Irie H, Honda H, Shinozaki K, et al. MR imaging of ampullary carcinomas. *J Comput Assist Tomogr* 2002;26(5):711–717.
90. Tublin ME, Moser AJ, Marsh JW, Gamblin TC. Biliary inflammatory pseudotumor: imaging features in seven patients. *AJR Am J Roentgenol* 2007;188(1):W44–W48.
91. Fujita T, Kojima M, Kato Y, et al. Clinical and histopathological study of “follicular cholangitis”: sclerosing cholangitis with prominent lymphocytic infiltration masquerading as hilar cholangiocarcinoma. *Hepatol Res* 2010;40(12):1239–1247.
92. Soto JA, Alvarez O, Lopera JE, Múnera F, Restrepo JC, Correa G. Biliary obstruction: findings at MR cholangiography and cross-sectional MR imaging. *RadioGraphics* 2000;20(2):353–366.

93. Masci E, Toti G, Mariani A, et al. Complications of diagnostic and therapeutic ERCP: a prospective multicenter study. *Am J Gastroenterol* 2001;96(2):417-423.
94. Andriulli A, Loperfido S, Napolitano G, et al. Incidence rates of post-ERCP complications: a systematic survey of prospective studies. *Am J Gastroenterol* 2007;102(8):1781-1788.
95. Al-Mofleh IA, Aljebreen AM, Al-Amri SM, et al. Biochemical and radiological predictors of malignant biliary strictures. *World J Gastroenterol* 2004;10(10):1504-1507.
96. Saluja SS, Sharma R, Pal S, Sahni P, Chattopadhyay TK. Differentiation between benign and malignant hilar obstructions using laboratory and radiological investigations: a prospective study. *HPB (Oxford)* 2007;9(5):373-382.
97. Park MS, Kim TK, Kim KW, et al. Differentiation of extrahepatic bile duct cholangiocarcinoma from benign stricture: findings at MRCP versus ERCP. *Radiology* 2004;233(1):234-240.
98. Ferrucci JT. MRI and MRCP in pancreaticobiliary malignancy. *Ann Oncol* 1999;10(suppl 4):18-19.
99. Souftas V, Kozadinos A, Mantatzis M, Prassopoulos P. The use of CT or MRI for the one-stage placement of stents in biliary obstructions. *Diagn Interv Radiol* 2010;16(3):241-244.

This journal-based SA-CME activity has been approved for AMA PRA Category 1 Credit™. See www.rsna.org/education/search/RG.

Adult Bile Duct Strictures: Role of MR Imaging and MR Cholangiopancreatography in Characterization

Venkata S. Katabathina, MD • Anil K. Dasyam, MD • Navya Dasyam, MBBS • Keyanoosh Hosseinzadeh, MD

RadioGraphics 2014; 34:565–586 • Published online 10.1148/rg.343125211 • Content Codes:   

Page 566

Either rapid acquisition with relaxation enhancement (RARE) or a variant thereof (eg, single-shot fast spin-echo, half-Fourier acquisition single-shot turbo spin-echo, or fast-recovery fast spin-echo) is used for MR cholangiopancreatography.

Page 572

IgG4 sclerosing disease can result in four different patterns of biliary strictures: (a) stricture of the distal CBD, (b) diffuse strictures of the intra- and extrahepatic bile ducts, (c) hilar stricture and distal CBD stricture, and (d) isolated hilar stricture.

Page 575

MR cholangiopancreatographic findings of RPC include intra- or extrahepatic bile duct stones, multiple intrahepatic biliary strictures, short-segment focal extrahepatic bile duct stricture, localized dilatation of lobar or segmental bile ducts with a predilection for the lateral segment of the left lobe and the posterior segment of the right lobe, bile duct wall thickening, abrupt tapering, and decreased arborization of the intrahepatic ducts.

Page 579

Identification of an ampullary mass, papillary bulging, irregular asymmetric luminal narrowing of the distal CBD, and diffuse upstream intra- and extrahepatic biliary dilatation are signs of malignant ampullary obstruction, whereas smooth symmetric luminal narrowing of the CBD and central biliary dilatation without an ampullary mass or papillary bulging are expected with a benign obstruction.

Pages 582–583

Kim et al showed that a narrowed segment with the following MR imaging features is more likely to be malignant: hyperenhancement relative to the liver during the portal venous phase, length of over 12 mm, wall thickness greater than 3 mm, indistinct outer margin, luminal irregularity, and asymmetry.